The kinases MSK1 and MSK2 act as negative regulators of Toll-like receptor signaling

Ananieva, Olga; Darragh, Joanne; Johansen, Claus; Carr, Julia M.; McIlrath, Joanne; Park, Jin Mo

Published in:
Nature Immunology

DOI:
10.1038/ni.1644

Publication date:
2008

Document Version
Peer reviewed version

MSK1 and MSK2 act as negative regulators of Toll-like receptor signalling.

Olga Ananieva, Joanne Darragh, Claus Johansen[1], Julia M. Carr, Joanne McIlrath, Jin Mo Park[2], Andrew Wingate, Claire E. Monk, Rachel Toth, Susana G. Santos, Lars Iversen[1] and J. Simon C. Arthur[*]

MRC Protein Phosphorylation Unit, School of Life Sciences, University of Dundee, Dow St., Dundee, DD1 5EH, UK

1 Department of Dermatology, Aarhus University Hospital, Aarhus, Denmark

2 Cutaneous Biology Research Center, Massachusetts General Hospital and Harvard Medical School, Charlestown, MA 02129, USA

Correspondence should be addressed to J.S.C.A (j.s.c.arthur@dundee.ac.uk).

Nature Immunology 9, 1028 - 1036 (2008)
Published online: 10 August 2008 | doi:10.1038/ni.1644
http://www.nature.com/ni/journal/v9/n9/full/ni.1644.html

Abstract

MSK1 and MSK2 kinases are activated downstream of the p38 and ERK1/2 MAPK kinases. Here we found that MSK1 and MSK2 are required to limit the production of pro-inflammatory cytokines in response to lipopolysaccharide (LPS) stimulation of primary macrophages. By inducing transcription of the MAPK phosphatase DUSP1 and the anti-inflammatory cytokine interleukin-10, MSK1,2 exert multiple negative feedback mechanisms. Deficiency of MSK1 and MSK2 prevented binding of phosphorylated transcription factors CREB and ATF1 to the *Il10* and *Dusp1* promoters. MSK1,2 double knockout mice were hypersensitive to LPS-induced endotoxic shock and showed prolonged inflammation in a PMA-induced toxic contact eczema model. These results establish MSK1 and MSK2 as key components of negative feedback mechanisms required to limit Toll-like receptor-driven inflammation.

Introduction

The innate immune system recognises pathogens via the detection of specific fungal, microbial or viral molecules referred to as pathogen associated molecular patterns (PAMPs). Several groups of receptors for PAMPs have been described, including Toll like receptors (TLRs), NOD like receptors and C-type lectins that recognize distinct sets of PAMPs[1-3].

In macrophages, a major consequence of TLR activation is the production of pro-inflammatory cytokines including tumor necrosis factor (TNF), interleukin (IL)-1, IL-6 and IL-12. The production of these cytokines is tightly controlled at the level of transcription, translation and secretion, and requires activation of several signalling pathways including those involving the transcription factor NF-κB and the MAP kinases (MAPK) ERK1/2, p38 and JNK[1-3]. The p38 pathway has attracted considerable interest as a possible target for anti-inflammatory drugs. Originally described as a lipopolysaccharide (LPS)-, stress- or IL-1–activated MAPK[4-6], p38 is the cellular target of a group of pyridinyl imidazole compounds that inhibit IL-1 and TNF production by monocytes[7]. Four p38 isoforms (p38α, p38β, p38γ and p38δ) have been described, but only p38α (http://www.signaling-gateway.org/molecule/query?afcsid=A001717) and p38β (http://www.signaling-gateway.org/molecule/query?afcsid=A001718) are inhibited by widely-used p38 inhibitors such as SB203580[8]. The use of gene-targeted mice revealed that p38α and not p38β plays critical roles in the innate immune system[9-11]. Whereas many p38 inhibitors have been developed as potential drugs for autoimmune disease, none have progressed through clinical trials due to problems with toxicity. Although it is possible that this toxicity is due to off target activity or inhibition of p38 outside the immune system, it is also possible that p38 inhibition could have unforeseen deleterious effects relating to the immune system[12,13].

In addition to their roles in promoting inflammation, TLRs can also activate negative feedback mechanisms and anti-inflammatory signals, which are critical in preventing excessive inflammation and may also play a role in the resolution of inflammation[12,14]. Several MAPKs including p38 and ERK1/2 are required for some of these negative feedback mechanisms, and it is possible that some of the toxicity of p38 MAPK inhibitors could be due to the inhibition of

these negative feedback pathways. For instance, p38 activation results in the phosphorylation of TAB1, the regulatory subunit of the complex containing TAK1, a MAP kinase kinase kinase (MAP3K) involved in the activation of p38, JNK and NF-κB resulting in inhibition of Tak1; thus p38 inhibition can result in enhanced JNK and NF-κB activity[15]. ERK1/2 and p38 also induce the transcription of DUSP1 (http://www.signaling-gateway.org/molecule/query?afcsid=A001547) (also known as mkp-1), a MAPK phosphatase that dephosphorylates and thus inactivates p38 and JNK *in vivo*[16]. Mice lacking DUSP1 exhibit prolonged p38 and JNK activation in response to LPS, as well as augmented TNF production and increased sensitivity to endotoxic shock[17-20].

MSK1 (http://www.signaling-gateway.org/molecule/query?afcsid=A001562) and MSK2 (http://www.signaling-gateway.org/molecule/query?afcsid=A001563) are two related kinases that are activated *in vivo* downstream of p38α and ERK1/2[21]. Mice that lack both MSK1 and MSK2 are viable and do not exhibit any obvious phenotype when maintained under specific pathogen free conditions[22]. MSK1,2 can phosphorylate the transcription factors CREB and ATF1, as well as the chromatin protein histone H3, in response to mitogens and cellular stress[22,23]. As a result, MSK1,2 are involved in the transcriptional induction of CREB-dependent immediate early genes[24,25]. Neurons lacking MSK1 show reduced transcription of DUSP1 after stimulation with neurotrophins[24]. If MSK1,2 also regulate DUSP1 transcription downstream of TLR signalling, they may play an anti-inflammatory role. Whereas TLR-induced MSK activation has been demonstrated in cell lines [21], the role of MSK1,2 in inflammation *in vivo* has not previously been addressed. We therefore used MSK1,2 double knockout mice to examine the role of MSKs downstream of TLR signalling both *in vivo* and in primary macrophages *in vitro*.

Results

MSKs in TLR-induced signaling

TLRs activate ERK1/2 and p38 in macrophages, suggesting that TLR signalling should also activate MSKs. LPS, via TLR4, activated ERK1/2 and p38α in bone marrow derived macrophages (BMDMs) (**Fig. 1a**). LPS also activated MSK1, as judged by phosphorylation of Thr581, a site important for MSK1 activation[21]. MSK1 activation was partially blocked by pre-incubation of the cells with inhibitors of MEK1/2 (PD184352, which blocks ERK1/2 activation[8]) or p38 (SB203580). A combination of both inhibitors was required to fully block MSK activation, indicating that both p38 and ERK1/2 contribute to TLR4-driven MSK activation (**Fig. 1a**). LPS also induced phosphorylation of CREB and histone H3.

To determine if MSKs were responsible for TLR4-induced CREB and histone H3 phosphorylation, we analyzed BMDMs from mice lacking MSK1 and MSK2. Deficiency of both MSK1 and MSK2 did not appear to makedly affect macrophage differentiation, as equivalent numbers of BMDMs were obtained from double knockout and wild-type controls, and wild-type and double knockout BMDMs expressed the macrophage-specific marker F4/80 and lacked the dendritic cell marker CD83 (**Supplementary Fig. 1**, online). However, LPS-driven phosphorylation of CREB and histone H3 was markedly reduced in double knockout BMDMs (**Fig. 1b**). This impaired phosphorylation was not due to an effect on upstream signalling, as double knockout BMDMs exhibited normal ERK1/2 and p38α phosphorylation in response to LPS (**Fig. 1b**). Similar results were obtained using the TLR ligands LTA (TLR2), Pam3CSK (TLR2, 1 and 6) and CpG DNA (TLR9) (**Fig. 1a,b**), indicating that the activation of MSK is not restricted to TLR4.

MSKs suppress pro-inflammatory cytokine production

As MSKs are activated by TLRs, we next examined the role of MSKs in pro-inflammatory cytokines by BMDMs using a cytokine multiplex array. Notably, MSK1,2 deficiency resulted in substantially elevated production of TNF, IL-6 and IL-12 (both IL-12p70 and IL-12p40) by LPS-

stimulated BMDMs (**Fig. 2a**). The increase in TNF was also observed by flow cytometry and immunoblotting for pre-TNF (**Fig. 2b**). No difference in the production of the other cytokines (IL-1α, IL-1β, IL-2, IL-3, IL-4, IL-5, IL-9, IL-13 and IL-17) in the array was seen between wild-type and double knockout cells (**Supplementary Fig. 2**, online).

Cytokine production in macrophages is regulated at several levels, including transcription, mRNA stability, translation and secretion. In the case of IL-12, MSK1,2 deficiency resulted in increased transcription of the genes encoding the p35 and p40 subunits at 6 and 8 hours after LPS stimulation (**Fig. 2c**). MSK1,2 deficiency exerted more moderate influence on TNF transcription, and influenced IL-6 transcription only after 8 hours of stimulation (**Fig. 2c**). The effects of MSK1,2 deficiency were in marked contrast to the effect of inhibiting p38 and ERK1/2 which, as expected, reduced TNF and IL-6 production in response to LPS (**Supplementary Fig. 3**, online). This finding would suggest that MSKs might be specifically involved in the activation of negative feedback pathways downstream of ERK1/2 and p38.

MSKs promote *Dusp1* transcription in macrophages.

Dusp1 is an immediate early gene encoding a MAPK phosphatase that promotes the deactivation of p38 following LPS stimulation, and DUSP1 deficiency results in elevated TNF production after TLR stimulation. In neurons, *Dusp1* transcription is regulated by MSKs via the phosphorylation of CREB[24]. Consistent with the finding that MSKs control CREB and ATF1 phosphorylation downstream of TLRs (**Fig. 1b**), we found that MSKs also promote *Dusp1* transcription in macrophages. DUSP1 mRNA was rapidly and transiently upregulated in response to LPS in wild-type BMDMs, and this upregulation was significantly lower in MSK1,2 double-knockout cells (**Fig. 3a**). Consistent with a role for MSK1, the transcription of *Dusp1* in BMDMs following LPS stimulation was not greatly affected by pre-incubation with either PD184352 or SB203580 alone; however, a combination of both PD184352 and SB203580 was able to inhibit DUSP1 mRNA induction (**Fig. 3b**). LPS stimulation also increased DUSP1

protein expression to a higher level in wild-type than MSK1,2 double knockout BMDMs (**Fig. 3c**).

In macrophages, DUSP1 preferentially dephoshorylates p38 rather than ERK1/2[17-20]. To test whether the decrease in DUSP1 protein expression in MSK1,2 double knockout cells affected MAPK signalling, phosphorylation of ERK1/2 and p38 was quantified over an extended time course of LPS stimulation. Deficiency of MSK1 and MSK2 had no effect on the time course of LPS-induced ERK1/2 phosphorylation (**Fig. 3c,d**). In contrast, MSK1,2 deficiency resulted in a slower dephosphorylation of p38 relative to that observed in wild-type cells (**Fig. 3c,d**). The partial nature of this effect likely stems from the fact that DUSP1 is not the only phosphatase for p38; overall, the pattern and magnitude of these results are in line with what has previously been reported in DUSP1-deficient macrophages[17-20].

MSKs drive IL-10 production

In addition to pro-inflammatory cytokines, LPS also triggers production of the anti-inflammatory cytokine IL-10 in macrophages. Previous studies implicated both ERK1/2 and p38 in IL-10 production[26]; consistent with these prior findings, DUSP1 deficiency results in increased IL-10 production in response to LPS[18].

In our studies, IL-10 mRNA quantities increased following LPS stimulation; however the magnitude of IL-10 mRNA induction was significantly lower in MSK1,2 double knockout than wild-type BMDMs (**Fig. 4a**). Consistent with a role for MSKs in *Il10* transcription, inhibition of p38 strongly inhibited LPS-mediated induction of both IL-10 mRNA expression and IL-10 sectertion (**Supplementary Fig. 4**, online). Notably, ERK1/2 inhibition caused an increase in IL-10 mRNA expression following LPS stimulation, suggesting that MAPK signalling can also influence *Il10* transcription independently of MSKs (**Supplementary Fig. 4**, online). Concentrations of secreted IL-10 steadily increased over an 8 hour time course after LPS stimulation of wild-type BMDMs (**Fig. 4b**). IL-10 secretion from LPS-stimulated MSK1,2 double knockout BMDMs was consistently lower than that released from wild-type BMDMs;

this discrepancy was most pronounced at early time points, as by 8 hours the amount of IL-10 released by double knockout cells reached 60% of the quantity produced by wild-type counterparts (**Fig. 4b**).

IL-10 inhibits the production of pro-inflammatory cytokines in macrophages, via the activation of Jak-STAT signalling. The importance of STAT3 in this process is highlighted by the finding that IL-10 does not effectively inhibit cytokine production in the absence of STAT3[27]. Stimulation of BMDMs with LPS for 2 to 8 hours induces STAT3 Tyr705 phosphorylation; this phosphorylation is likely the result of autocrine IL-10 production as it does not occur in IL-10–deficient mice[28]. Consistent with these findings we found that STAT3 phosphorylation induced by either 2 or 6 hours of LPS stimulation was blocked by an IL-10–neutralizing antibody (**Supplementary Fig. 5**, online). In line with the decreased IL-10 production from MSK1,2 double knockout BMDMs (**Fig. 4b**), LPS-induced STAT3 phosphorylation was lower in MSK1,2 double knockout compared to wild-type BMDMs after 2 hours of LPS stimulation; however similar STAT3 phosphorylation was seen in the double knockouts and wild-type cells at 6 and 8 hours after LPS stimulation (**Fig. 4c**). The effect of MSK1,2 deficiency on early LPS-triggered STAT3 phosphorylation was not due to a role of MSKs downstream of IL-10, as stimulation of BMDMs with IL-10 resulted in similar amounts of STAT3 phosphorylation as well as induction of SOCS3 mRNA—an established target of IL-10 signaling—in MSK1,2 double knockout and wild-type BMDMs (**Supplementary Fig. 5**, online). The normal STAT3 phosphorylation observed at later time points after LPS stimulation in the MSK1,2 double knockout BMDMs could be explained by STAT3 phosphorylation being induced by another cytokine, such as IL-6, which is produced in higher amounts by the MSK1,2 double knockout cells (**Fig. 2a**). Alternatively it could also be explained by the finding that by 8 h the double knockout BMDMs produced 60% of the IL-10 made by wild-type cells (**Fig. 4b**); perhaps this amount of IL-10 is sufficient to induce full STAT3 phosphorylation. To test these hypotheses, we used neutralizing antibodies against IL-10 and IL-6. IL-10– and IL-6–induced STAT3 phosphorylation was blocked by IL-10– and IL-6–neutralizing antibodies, respectively (**Fig. 4d**).

In both MSK1,2 double knockout and wild-type BMDMs the IL-10– but not the IL-6–neutralizing antibodies blocked STAT3 phosphorylation induced by 8 hours of LPS stimulation. These findings suggest that the amount of IL-10 released by MSK1,2 double knockout macrophages is sufficient to trigger full STAT3 phosphorylation at later time points after LPS stimulation.

Addition of exogenous IL-10 to macrophages inhibits the induction of pro-inflammatory cytokines in response to LPS[27]. We therefore used an IL-10–neutralizing antibody to block the action of endogenous IL-10 to determine if the difference in TNF, IL-6 and IL-12 production between wild-type and MSK1,2 double knockout BMDMs could be explained by the lower IL-10 production from the double knockout cells. In the absence of the IL-10–neutralizing antibody, MSK1,2 double knockout BMDMs produced more TNF, IL-6 and IL-12 mRNA and protein than wild-type BMDMs following LPS treatment. Addition of anti–IL-10 resulted in only a moderate increase in LPS-driven production of TNF, IL-6 and IL-12 in MSK1,2 double knockout BMDMs, but a substantial augmentation of LPS-driven IL-6 and IL-12 cytokine production in wild-type BMDMs (**Fig. 5e,f**). TNF secretion was also increased by anti–IL-10 in wild-type BMDMs; however unlike IL-6 and IL-12 the increased TNF did not approach the quantity secreted by MSK1,2 double knockout macrophages (**Fig. 5e,f**). No effect was seen when an isotope control antibody was used (**Fig. 5e,f**), and the anti–IL-10 treatment did not significantly affect LPS-induced IL-10 production by either wild-type or MSK1,2 double knockout BMDMs (**Supplementary Fig. 6**, online).

To confirm the results with the IL-10–neutralizing antibody, MSK1,2 double knockout mice were crossed onto an IL-10–deficient background. As expected, IL-10–deficient BMDMs secreted more IL-12, IL-6 and TNF than wild-type cells in response to LPS (**Fig. 5g**). IL-10–deficient and MSK1,2,IL-10 triple knockout BMDMs showed little difference in LPS-driven IL-6 and IL-12 production (**Fig. 5g**). Together these results indicate that the lower IL-10 production by MSK1,2 double knockout BMDMs strongly contributed to the higher IL-6 and IL-12 production by MSK1,2 double knockout BMDMs. In contrast to IL-6 and IL-12, TNF amounts

produced by MSK1,2,IL-10 triple knockout BMDMs were higher than that released by IL-10–deficient BMDMs (**Fig. 5g**), consistent with the IL-10–neutralizing antibody results . Together, these findings indicate that MSKs regulate TNF production via IL-10–dependent and IL-10–independent mechanisms.

CREB and ATF1 in *Dusp1* and *Il10* transcription

IL-10 and DUSP1 mRNA expression induced by LPS stimulation was significantly impaired in MSK1,2 double knockout BMDMs, suggesting that MSKs may directly control *Il10* and *Dusp1* promoters. MSKs phosphorylate CREB on Ser133 and thus increase its transcriptional activity. MSKs also phosphorylate ATF1, a CREB family member, on Ser63, a site with identical surrounding sequence to Ser133 in CREB. As CREB and ATF1 were phosphorylated by MSK1,2 after LPS stimulation (**Fig. 1b**), we investigated the influence of CREB and ATF1 on *Il10* and *Dusp1* transcription. Chromatin immunoprecipitation (ChIP) using an antibody that recognizes the phosphorylated forms of CREB and ATF1 showed that phosphorylated CREB and/or ATF1 were bound to the *Il10* and *Dusp1* promoters following LPS stimulation in wild-type but not MSK1,2 double knockout BMDMs (**Fig. 6a**).

To determine if the phosphorylation of CREB was essential for *Il10* and *Dusp1* transcription, gene targeted mice with a conditional Ser133Ala point mutation in the endogenous *CREB1* gene crossed to a Tamoxifen-inducible Cre transgenic were examined (**Supplementary Fig. 7a**, online). Mutation of CREB in BMDMs was induced by excision of a wild type minigene by addition of Tamoxifen. In the Ser133Ala CREB BMDMs residual CREB phophorylation was observed in response to LPS suggesting that some cells may have escaped excision of the minigene (**Fig. 6b**). Analysis of ERK1/2, p38 and MSK1 phosphorylation following LPS stimulation showed that the CREB S133A mutation did not affect the activation of these upstream signalling pathways (**Fig. 6b**). Expression of Egr1 mRNA (a transcript established to be independent of MSK1 and CREB)[22] as well as TNF and IL-6 mRNA, was not affected by the S133A mutation (**Supplementary Fig. 7b**, online). In contrast, expression of *Nur77*, a known

CREB-regulated MSK target gene[25], was reduced in S133A BMDMs (**Fig. 6c**). Consistent with what was observed in MSK1,2 double knockout BMDMs, S133A BMDMs showed impaired LPS-induced expression of IL-10 mRNA; however, CREB mutation did not alter DUSP1 mRNA expression (**Fig. 6c**). These results show that MSKs promotes *Il10* transcription via the phosphorylation of CREB, and suggest that *Dusp1* transcription may be regulated by the phosphorylation of ATF1 by MSKs.

MSK1,2 influence in inflammatory models

Intraperitoneal (i.p) injection of LPS in mice can lead to endotoxic shock and mortality. Based on the effects of MSK1,2 deficiency on LPS responses in BMDMs described above, we would predict that MSK1,2 deficient mice would be more sensitive to LPS-induced endotoxic shock than wild-type mice. To test this hypothesis, mice were given a sublethal dose of LPS, and their body temperature monitored over time. A drop of 2^{o}C in body temperature was taken as predictive of the development endotoxic shock and probable mortality[29], and the mice were humanely sacrificed at this point. Injection of LPS (2.5 mg/kg) into wild-type mice did not result in any substantial drop in body temperature over a 24 hour time course, and the mice did not exhibit any severe signs of LPS-induced toxicity. In contrast, injection of the same amount of LPS into MSK1,2 double knockout mice resulted in obvious signs of LPS-induced toxicity, including piloerection, diarrhoea, eye inflammation, and a substantial drop in body temperature within 4 to 8 hours of LPS injection (**Fig. 7a**); all LPS-injected MSK1,2 double knockout mice exhibited a pathology of a severity that necessitated sacrifice during this time interval. In similar experiments, mice were injected with a lower dose of LPS (1.8 mg/kg), and plasma cytokine concentrations were measured after 1 and 4 hours. In wild-type mice, plasma TNF concentrations peaked at 1 hour after stimulation, but decreased towards baseline after 4 hours. Interestingly, TNF concentrations 1 hour after LPS injection were approximately 7-fold higher in MSK1,2 double knockout mice compared to wild-type animals (**Fig. 7b**). In contrast to TNF, IL-6 and IL-12 were only marginally increased in wild-type animals by 1 h, but were markedly elevated at the 4 hour time point. Both IL-6 and IL-12 were significantly higher in MSK1,2

double knockout compared to wild-type mice 4 hours following LPS injection (**Fig. 7b**). Similar to the observations made in BMDMs, substantially lower concentrations of IL-10 were present in the plasma of MSK1,2 double knockout mice compared to wild-type mice following LPS injection (**Fig. 7b**). No difference in plasma concentrations of IL-1α, IL-1β, IL-2, IL-3, IL-4, IL-5, IL-9, IL-13 and IL-17 were seen between wild-type and MSK1,2 double knockout mice (**Supplementary Fig. 8**, online). Together these results show that MSK deficiency increases sensitivity of mice to LPS-induced endotoxic shock, and these findings correlate with the elevated TNF, IL-6 and IL-12 and decreased IL-10 amounts in MSK1,2 double knockout mice.

Whereas i.p. injection of LPS has some similarities to septic shock, clinical sepsis is a much more complex condition and several major differences between the two conditions have been described[30]. As the cecal ligation and puncture (CLP) model shows more similarities to septic shock in humans[30], the effect of MSK1,2 deficiency was also examined in this system. In these experiments, wild-type and double knockout mice showed similar mortality or morbity within 8 hours of CLP (6/10 double knockout and 5/10 WT died). However, after 48 hours, all remaining double knockout mice, but only 1 wild-type mouse survived (**Fig. 7c**). In a separate experiment, plasma cytokine concentrations were measured at 1 and 4 hours after CLP. In contrast to i.p. LPS injection, CLP induced little expression of TNF at this time point. Similarly, IL-12 expression increased only 4 to 6 fold and was not markedly affected by knockout of MSK1 and MSK2 (**Fig. 7d**). IL-6 was strongly induced by CLP, but also was not substantially affected by MSK1,2 deficiency (**Fig. 7d**). IL-10 was also induced by CLP in wild-type animals and, consistent with the i.p. LPS model, double knockout animals expressed less IL-10 (**Fig. 7d**).

The consequence of MSK1,2 deficiency was also examined in an acute PMA-induced toxic contact eczema model. In this model local inflammation is induced in the ear by topical administration of PMA. In wild-type mice, this localized inflammation results in an increase in ear thickness, which normally peaks at 8 hours and then slowly resolves (**Fig. 8a**). In MSK1,2 double knockout mice the inflammation failed to resolve, and no substantial reduction in ear thickness was seen even by 96 hours after PMA treatment (**Fig. 8a**). The extent of neutrophil

recruitment was estimated using an MPO (myeloperoxidase) assay on extracts from ear biopsies. Consistent with the lack of resolution of ear thickness, MPO activity was significantly increased in the MSK1,2 double knockout compared to wild-type animals, at both 72 and 96 hours after PMA treatment (**Fig. 8b**). Histological analysis of the inflamed tissue confirmed an increased cellular infiltration in the dermis, as well as an increased total ear and epidermal thickness, in MSK1,2 double knockout compared to wild-type animals (**Fig. 8c**).

These results suggest that MSK have a protective role in acute endotoxic shock and toxic contact eczema, but may have a deleterious function in sepsis.

Discussion

Although ERK1/2 and p38 have previously been shown to play important roles in pro-inflammatory cytokine production and inflammation, it is now becoming apparent that these MAP kinases also activate negative feedback pathways that are critical for preventing uncontrolled inflammation. This negative feedback occurs through both intracellular mechanisms and via the release of anti-inflammatory cytokines. For instance, p38 is able to inhibit the MAP3K TAK1 via phosphorylation of the regulatory subunit TAB1[15], whereas both ERK1/2 and p38 can induce the expression of DUSP1 that promotes the inactivation of p38 and JNK[17-20]. In addition, both ERK and p38 promote expression of tristetraprolin (TTP), which induces degradation of TNF mRNA[31]. TLR signalling also induces the production of IL-10, an anti-inflammatory cytokine known to inhibit pro-inflammatory cytokine production by macrophages[27].

Here we show that the ERK1/2- and p38- activated kinases MSK1 and MSK2 utilize multiple mechanisms to limit the pro-inflammatory effect of TLR4 signalling. Knockout of MSK1 and MSK2 resulted in decreased expression of DUSP1. The *Dusp1* promoter contains a conserved CREB-binding site[32], *Dusp1* is a CREB-dependent immediate early gene in neurons[24], and knockout of MSK1 blocks CREB phosphorylation and *Dusp1* transcription in response to brain-derived neurotrophic factor (BDNF) in cortical neurons. Using ChIP analysis, we found that phosphorylated CREB and/or ATF1 binds to the *Dusp1* promoter following LPS stimulation in

BMDMs, in a manner dependent on MSK activity. Notably, phosphorylation of CREB on Ser133 was not essential for *Dusp1* transcription in response to LPS; this observation suggests that MSK1,2 regulate the *Dusp1* promoter via the phosphorylation of ATF1, or by an undescribed mechanism.

Similar to MSK1,2 double knockout mice, DUSP1-deficient mice do not show an obvious phenotype in the absence of LPS challenge, but like MSK1,2 double knockouts, DUSP1-knockouts do show increased susceptibility to LPS-induced endotoxic shock[17-20]. Whereas the phenotype of the DUSP1-deficient and MSK1,2-deficient animals are similar, the reduction in DUSP1 expression alone is unlikely to explain all the effects seen in the MSK1,2 double knockout animals. A major difference between the two animal models is in the expression of IL-10, which is decreased in MSK1,2 double knockout but increased in DUSP1-deficient mice. As LPS-induced IL-10 production was reduced by inhibition of p38, the elevated IL-10 concentrations in the DUSP1 knockouts are consistent with the prolonged p38 activation in these mice. In contrast, the reduction of LPS-induced IL-10 transcription in the MSK1,2 double knockouts, together with the lack of reduction in ERK1/2 and p38 activation, suggests that MSKs may directly regulate the transcription of IL-10. Consistent with this, two MSK substrates, CREB and histone H3, have been proposed to be involved in *Il10* transcription[26,33-35]. In BMDMs, MSKs were required for binding of phosphorylated CREB and/or ATF1 to the *Il10* promoter following LPS stimulation, and that mutation of the Ser133 phosphorylation site in endogenous CREB reduced *Il10* transcription in response to LPS.

MSK1,2 deficiency also resulted in elevated production of TNF, IL-6 and IL-12 at later time points after LPS stimulation. As MSK1,2 double knockout and wild-type cells produced similar amounts of IL-6 and IL-12 in the presence of an IL-10–neutralizing antibody, and as MSK1,2 deficiency had little effect on IL-6 and IL-12 production on an IL-10–deficient background, MSK1,2 seem to regulate IL-6 and IL-12 via an autocrine inhibition loop involving IL-10. In contrast, augmented TNF production in MSK1,2 double knockouts seems to be the result of IL-10-dependent and independent mechanisms. Increased p38 activation, due to the reduction in

DUSP1 expression, may be involved. In addition, MSK-mediated regulation of the transcription of TTP, an mRNA binding protein that destabilises TNF mRNA, might play a role[31].

The role of MSK was not limited to BMDMs, as similar results were obtained in *in vivo* models of endotoxic shock and eczema where MSK1,2 deficiency resulted in increased inflammation. MSK1,2 double knockouts, however, did not show an increased sensitivity in the CLP model. This may be due to CLP being a more acute model than the i.p. Injection of a low dose LPS making it more difficult to observe an increase in sensitivity. Surprisingly while there was a similar mortality in the wild type and knockout mice before excision of the caceum, after excision no mortality occurred in the knockout animals while all but one of the remaining wild type animals were terminated. This suggests that MSK knockout could be protective in sepsis, but deleterious in acute endotoxic shock. Many differences have been described between these two models, making it difficult to directly extrapolate findings from one model to the other. In contrast to i.p. LPS injection, CLP induces a bacterial peritonitis that activates a wider range of immune pathways and involves both inflammatory and immunosuppressive stages [30]. Relevant to this it has been shown that CLP is not affected by loss of TLR4 (the receptor for LPS), indicating that several PAMPs are important in this model[36,37]. The role of cytokines in the two models is also different, for instance TNF blockade is protective following LPS injection but not in CPL[38]. In fact endogenous TNF has been suggested to have protective effects under some circumstances in CLP; TNF neutralising antibodies have a harmfull effect if administered immediately after CLP[39], and TNF-Receptor1 knockout mice show higher mortality in a CLP model[40].

The role of IL-10 is also complex. Neutralisation of IL-10 with antibodies prior to induction of CLP[41] or IL-10 knockout[42] increases mortality in CLP. In contrast, blocking IL-10 after the induction of CLP (a situation more similar to what would occur in the MSK1,2 double knockout), either by neutralising antibodies[43] or inhibition of IL-10 transcription[44] had a protective effect. In addition, high IL-10 levels have been correlated with poor outcome in clinical sepsis[45].

IL-12 is another cytokine that was increased in MSK knockouts following LPS stimulation. IL-12 knockout mice[46] or IL-12 neutralising antibodies[47] both sensitise mice to mortality in CLP. One possible explanation for the CPL results in the MSK knockout mice is that MSK has an immunosuppressive effect that may reduce bacterial clearance resulting in increased peritonitis. Together these results establish the critical role played by MSK1,2 in limiting pro-inflammatory signalling downstream of TLRs. It is possible that some of the toxicity associated with p38 inhibitors could be due to the inhibition of MSK1,2-mediated negative feedback mechanisms.

Thus, agents that selectively activate MSK1,2 may have therapeutic benefits in situations where increased IL-10 and reduced pro-inflammatory cytokine production is desired.

Methods

Animals

Mice lacking MSK1 and MSK2 have been described previously[22]. IL-10–deficient mice[48] on a C57/Bl6 background were obtained from the Jackson Labs. An inducible S133A mutation in the endogenous CREB gene was generated via the insertion of a floxed minigene (**Supplementary Fig. 7**, online) and will be reported elsewhere. To allow the generation the CREB knockin mutation in BMDMs, these mice were crossed onto a Tamoxifen inducible CRE strain. The Tamoxifen inducible CRE transgene was found to have no effect on LPS induced CREB phosphorylation or cytokine transcription (**Supplementary Fig. 9**, online)All strains were backcrossed on to C57Bl6 for a minimum of 6 generations. Mice were housed under specific pathogen-free condition in accordance with EU regulations. Work was approved by local ethical review and carried out under either a UK Home Office project licence (in vivo LPS injection) or were approved by the Danish Laboratory Animal Research committee (Dyreforsøgstilsynet) (j/nr 2005/561-963) (CLP, Acute toxic contact eczema).

Cell culture

BMDMs were isolated from the femurs of adult mice as described previously[10]. BM cells were differentiated on bacterial grade plastic dishes for 7 days in DMEM supplemented with 10% FBS, 100 units/ml Penicillin, 100 µg/ml Streptomycin, 0.25 µg/ml Amphothericin B, 5 mg/ml L-Glutamine, and 5 ng/ml M-CSF (R&D). Where appropriate, the CREB S133A mutation was induced by the addition of 0.1 µM Tamoxifen on day 5 of cultures. After 7 days adherent cells were removed using Versene solution (Gibco), counted and re-plated at constant density (2×10^5 cells/ml). Cells were stimulated for the indicated times 24 to 48 h after re-plating using either 100 ng/ml LPS (Sigma), of Pam3CSK4 (1 µg/ml), LTA-SA (5 µg/ml) or CpG DNA (ODN1826, 2.5 µM), all from InvivoGen. For experiments using kinase inhibitors, either PD184352 (2 µM/ml) or SB203580 (5 µM/ml) were added to the culture media 1 hour before stimulation. For immunoblotting cells were lysed directly into 1% (w/v) SDS sample buffer. For RNA, cells

were lysed in an RNA lysis buffer (Qiagen) and RNA isolated using Qiagen RNAeasy® Microkit.

***In vivo* LPS injection**

Mice (6-8 weeks old) were injected with LPS (Sigma, 1.8 mg/kg) intraperitoneally (i.p.). Mice were sacrificed one hour or four hours after the LPS injection and plasma samples were collected for cytokine analysis.

Cecal ligation and puncture

Mice (7-8 weeks old) were starved for 16 h and cecum was ligated just below the ileocecal valve maintaining bowel continuity[49]. The cecum was punctured at both ends using a 21G needle and a single droplet of fecal material was extruded from each puncture site. The abdomen was closed in two layers, resuscitated subcutaneously with 3 ml/100 g BW saline, a microchip inserted subcutaneously on the back of the mouse and the animal returned to its cage; this was taken as time 0 for subsequent measurements. After 10 hours, the cecum was excised and the abdominal cavity irrigated with warm saline. The abdominal cavity was closed and animals resuscitated subcutaneously with 3 ml/100 g BW saline. A blood sample was taken after 6 hours, and animals were resuscitated subcutaneously with 3 ml/100 g BW saline every 10 hours. The temperature of the mice was measured at the indicated time points. If a drop in body temperature below 30^{o}C was observed in a moribund animal, or if a prolonged drop below 30^{o}C was observed for several hours, the animals were humanely sacrificed. In a similar experiment, 100 µl of blood was taken at 1 h, followed by termination of the animal at 4 h allowing a further blood sample to be taken. Plasma cytokine levels were then measured in the blood samples using Luminex assays. The CLP model was performed by Pipeline biotech A/S.

LPS-induced endotoxic shock

Mice (10-12 weeks old) were anaesthetised and temperature sensors were surgically implanted into the peritoneal cavity. 14 days later mice were challenged with 2.5 mg/kg of LPS (Sigma), i.p. Temperatures of mice were monitored constantly after the LPS injection using Remo 400 detection system. A drop in the temperature of more than 1.5-2°C compared to the average

diurnal temperature was used as an indicative of LPS-induced death and the mice were sacrificed.

Acute toxic contact eczema model

Mice (6-8 week old males) were treated with phorbol 12-myristate 13-acetate (PMA) (Sigma) on the ears (2.5 µg/ear). Ear thickness was measured before the first challenge of PMA and again post-challenge at the times indicated, using a Mitutyo digimatic indicator. The mice were anaesthetized during the ear measurement.

Myeloperoxidase (MPO) assay

Four mm punch biopsies were taken from the ears of the mice 72 and 96 h after PMA challenge and immediately placed in liquid nitrogen. The MPO assay was carried out as previously described[50]. Briefly, the biopsies were homogenised in 200 µl 0.5% hexadecyltrimethylammonium bromide (HTAB). Samples were incubated at 37°C for 1 hour and then centrifuged for 5 min. MPO activity was assayed in the supernatant as follows; 20 µl of the supernatant was added to 96-well plates containing 100 µl of TMB ONE, Ready-to-use Substrate (Kem-En-Tec Diagnostics A/S). After 10 min incubation in the dark at room temperature the reaction was stopped by adding 100 µl 0.2 M H_2SO_4. Results were determined by an ELISA reader (Laboratory Systems iEMS Reader MF) at 450 nm. A standard curve was constructed with polymorphonuclear human cells (PMNs) obtained from blood from healthy human volunteers. PNMMNs were prepared using Polymorphprep^{TM} (AXIS-SHIELD PoC AS) according to the manufacturer's instructions. These experiments were approved by the local ethical commitee of Aarhus and undersigned informed consent was obtained from the volunteers.

Other methods

Details of antibodies, chromatin immunoprecipitation, quantative PCR, cytokine assay, FACS and histology are provided in the supplementary methods online.

Acknowledgements

This research was supported by grants from the UK Medical Research Council, Arthritis Research Campaign, Astra-Zeneca, Boehringer-Ingelheim, GlaxoSmithKline, Merck and Co, Merck KGaA and Pfizer. We would like to thank A. O'Garra (National Institute of Medical Research, London) for the gift of the neutralizing IL-10 antibody.

References

1. Kawai, T. & Akira, S. TLR signaling. *Semin Immunol* **19**, 24-32 (2007).
2. Miggin, S.M. & O'Neill, L.A. New insights into the regulation of TLR signaling. *J Leukoc Biol* **80**, 220-6 (2006).
3. Lee, M.S. & Kim, Y.J. Signaling pathways downstream of pattern-recognition receptors and their cross talk. *Annu Rev Biochem* **76**, 447-80 (2007).
4. Han, J., Lee, J.D., Bibbs, L. & Ulevitch, R.J. A MAP kinase targeted by endotoxin and hyperosmolarity in mammalian cells. *Science* **265**, 808-11 (1994).
5. Freshney, N.W. et al. Interleukin-1 activates a novel protein kinase cascade that results in the phosphorylation of Hsp27. *Cell* **78**, 1039-49 (1994).
6. Rouse, J. et al. A novel kinase cascade triggered by stress and heat shock that stimulates MAPKAP kinase-2 and phosphorylation of the small heat shock proteins. *Cell* **78**, 1027-37 (1994).
7. Cuenda, A. et al. SB 203580 is a specific inhibitor of a MAP kinase homologue which is stimulated by cellular stresses and interleukin-1. *FEBS Lett* **364**, 229-33 (1995).
8. Bain, J. et al. The selectivity of protein kinase inhibitors: a further update. *Biochem J* **408**, 297-315 (2007).
9. O'Keefe, S.J. et al. Chemical Genetics Define the Roles of p38{alpha} and p38 in Acute and Chronic Inflammation. *J Biol Chem* **282**, 34663-71 (2007).
10. Beardmore, V.A. et al. Generation and characterization of p38beta (MAPK11) gene-targeted mice. *Mol Cell Biol* **25**, 10454-64 (2005).
11. Kang, Y.J. et al. Macrophage deletion of p38alpha partially impairs lipopolysaccharide-induced cellular activation. *J Immunol* **180**, 5075-82 (2008).
12. Lang, T. & Mansell, A. The negative regulation of Toll-like receptor and associated pathways. *Immunol Cell Biol* **85**, 425-34 (2007).
13. Dambach, D.M. Potential adverse effects associated with inhibition of p38alpha/beta MAP kinases. *Curr Top Med Chem* **5**, 929-39 (2005).
14. Liew, F.Y., Xu, D., Brint, E.K. & O'Neill, L.A. Negative regulation of toll-like receptor-mediated immune responses. *Nat Rev Immunol* **5**, 446-58 (2005).
15. Cheung, P.C., Campbell, D.G., Nebreda, A.R. & Cohen, P. Feedback control of the protein kinase TAK1 by SAPK2a/p38alpha. *Embo J* **22**, 5793-805 (2003).
16. Chen, P. et al. Restraint of proinflammatory cytokine biosynthesis by mitogen-activated protein kinase phosphatase-1 in lipopolysaccharide-stimulated macrophages. *J Immunol* **169**, 6408-16 (2002).
17. Salojin, K.V. et al. Essential role of MAPK phosphatase-1 in the negative control of innate immune responses. *J Immunol* **176**, 1899-907 (2006).
18. Chi, H. et al. Dynamic regulation of pro- and anti-inflammatory cytokines by MAPK phosphatase 1 (MKP-1) in innate immune responses. *Proc Natl Acad Sci U S A* **103**, 2274-9 (2006).
19. Zhao, Q. et al. MAP kinase phosphatase 1 controls innate immune responses and suppresses endotoxic shock. *J Exp Med* **203**, 131-40 (2006).

20. Hammer, M. et al. Dual specificity phosphatase 1 (DUSP1) regulates a subset of LPS-induced genes and protects mice from lethal endotoxin shock. *J Exp Med* **203**, 15-20 (2006).
21. Arthur, J.S. MSK activation and physiological roles. *Front Biosci* **13**, 5866-5879 (2008).
22. Wiggin, G.R. et al. MSK1 and MSK2 are required for the mitogen- and stress-induced phosphorylation of CREB and ATF1 in fibroblasts. *Mol Cell Biol* **22**, 2871-81 (2002).
23. Soloaga, A. et al. MSK2 and MSK1 mediate the mitogen- and stress-induced phosphorylation of histone H3 and HMG-14. *Embo J* **22**, 2788-97 (2003).
24. Arthur, J.S. et al. Mitogen- and stress-activated protein kinase 1 mediates cAMP response element-binding protein phosphorylation and activation by neurotrophins. *J Neurosci* **24**, 4324-32 (2004).
25. Darragh, J. et al. MSKs are required for the transcription of the nuclear orphan receptors Nur77, Nurr1 and Nor1 downstream of MAPK signalling. *Biochem J* **390**, 749-59 (2005).
26. Zhang, X., Edwards, J.P. & Mosser, D.M. Dynamic and transient remodeling of the macrophage IL-10 promoter during transcription. *J Immunol* **177**, 1282-8 (2006).
27. Murray, P.J. Understanding and exploiting the endogenous interleukin-10/STAT3-mediated anti-inflammatory response. *Curr Opin Pharmacol* **6**, 379-86 (2006).
28. Carl, V.S., Gautam, J.K., Comeau, L.D. & Smith, M.F., Jr. Role of endogenous IL-10 in LPS-induced STAT3 activation and IL-1 receptor antagonist gene expression. *J Leukoc Biol* **76**, 735-42 (2004).
29. Stiles, B.G., Campbell, Y.G., Castle, R.M. & Grove, S.A. Correlation of temperature and toxicity in murine studies of staphylococcal enterotoxins and toxic shock syndrome toxin 1. *Infect Immun* **67**, 1521-5 (1999).
30. Rittirsch, D., Hoesel, L.M. & Ward, P.A. The disconnect between animal models of sepsis and human sepsis. *J Leukoc Biol* **81**, 137-43 (2007).
31. Brook, M. et al. Posttranslational regulation of tristetraprolin subcellular localization and protein stability by p38 mitogen-activated protein kinase and extracellular signal-regulated kinase pathways. *Mol Cell Biol* **26**, 2408-18 (2006).
32. Sommer, A., Burkhart, H., Keyse, S.M. & Luscher, B. Synergistic activation of the mkp-1 gene by protein kinase A signaling and USF, but not c-Myc. *FEBS Lett* **474**, 146-150 (2000).
33. Platzer, C. et al. Cyclic adenosine monophosphate-responsive elements are involved in the transcriptional activation of the human IL-10 gene in monocytic cells. *Eur J Immunol* **29**, 3098-104 (1999).
34. Saraiva, M. et al. Identification of a macrophage-specific chromatin signature in the IL-10 locus. *J Immunol* **175**, 1041-6 (2005).
35. Park, J.M. et al. Signaling pathways and genes that inhibit pathogen-induced macrophage apoptosis--CREB and NF-kappaB as key regulators. *Immunity* **23**, 319-29 (2005).
36. Echtenacher, B., Freudenberg, M.A., Jack, R.S. & Mannel, D.N. Differences in innate defense mechanisms in endotoxemia and polymicrobial septic peritonitis. *Infect Immun* **69**, 7271-6 (2001).
37. Peck-Palmer, O.M. et al. Deletion of MyD88 markedly attenuates sepsis-induced T and B lymphocyte apoptosis but worsens survival. *J Leukoc Biol* **83**, 1009-18 (2008).
38. Riedamann, N.C., Guo, R. & Ward, P.A. The enigma of sepsis. *Journal Clinical Investigation* **112**, 460-467 (2003).
39. Echtenacher, B., Falk, W., Mannel, D.N. & Krammer, P.H. Requirement of endogenous tumor necrosis factor/cachectin for recovery from experimental peritonitis. *J Immunol* **145**, 3762-6 (1990).
40. Hildebrand, F., Pape, H.C., Hoevel, P., Krettek, C. & van Griensven, M. The importance of systemic cytokines in the pathogenesis of polymicrobial sepsis and dehydroepiandrosterone treatment in a rodent model. *Shock* **20**, 338-46 (2003).
41. van der Poll, T. et al. Endogenous IL-10 protects mice from death during septic peritonitis. *J Immunol* **155**, 5397-401 (1995).

42. Latifi, S.Q., O'Riordan, M.A. & Levine, A.D. Interleukin-10 controls the onset of irreversible septic shock. *Infect Immun* **70**, 4441-6 (2002).
43. Song, G.Y., Chung, C.S., Chaudry, I.H. & Ayala, A. What is the role of interleukin 10 in polymicrobial sepsis: anti-inflammatory agent or immunosuppressant? *Surgery* **126**, 378-83 (1999).
44. Kalechman, Y. et al. Anti-IL-10 therapeutic strategy using the immunomodulator AS101 in protecting mice from sepsis-induced death: dependence on timing of immunomodulating intervention. *J Immunol* **169**, 384-92 (2002).
45. Gogos, C.A., Drosou, E., Bassaris, H.P. & Skoutelis, A. Pro- versus anti-inflammatory cytokine profile in patients with severe sepsis: a marker for prognosis and future therapeutic options. *J Infect Dis* **181**, 176-80 (2000).
46. Moreno, S.E. et al. IL-12, but not IL-18, is critical to neutrophil activation and resistance to polymicrobial sepsis induced by cecal ligation and puncture. *J Immunol* **177**, 3218-24 (2006).
47. Steinhauser, M.L., Hogaboam, C.M., Lukacs, N.W., Strieter, R.M. & Kunkel, S.L. Multiple roles for IL-12 in a model of acute septic peritonitis. *J Immunol* **162**, 5437-43 (1999).
48. Kuhn, R., Lohler, J., Rennick, D., Rajewsky, K. & Muller, W. Interleukin-10-deficient mice develop chronic enterocolitis. *Cell* **75**, 263-274 (1993).
49. Hubbard, W.J. et al. Cecal ligation and puncture. *Shock* **24 Suppl 1**, 52-7 (2005).
50. Ottosen, E.R. et al. Synthesis and structure-activity relationship of aminobenzophenones. A novel class of p38 MAP kinase inhibitors with high antiinflammatory activity. *J Med Chem* **46**, 5651-62 (2003).

Figure 1 MSK is activated by TLR signalling

A) Wild-type BMDMs were pre-incubated for 1 h with PD184352 (2 μM), SB203580 (5 μM) or a combination of both inhibitors as indicated, and were then stimulated for 30 min with either LPS (100 ng/ml), Pam3CSK4 (Pam, 1 μg/ml), LTA-SA (LTA, 5 μg/ml) or CpG DNA (2.5 μM). Cells were lysed in SDS sample buffer and immunoblotted for p-MSK1(Thr581), p-CREB(Ser133), p-Histone H3(Ser10), p-ERK1/2, p-p38 and total p38. Results are representative of three independent experiments.

B) BMDMs were isolated from wild-type (WT) and MSK1,2 double knockout (KO) mice and were stimulated with LPS (100 ng/ml), Pam3CSK4 (Pam, 1 μg/ml), LTA-SA (LTA, 5 μg/ml) or CpG DNA (2.5 μM) for 15 or 30 min as indicated, then lysed and immunoblotted as in (**a**). Results are representative of three independent experiments.

Figure 2 MSK1,2 deficiency results in elevated pro-inflammatory cytokine production in response to LPS.

A) BMDMs from either wild-type (WT) or MSK1,2 double knockout (KO) mice were stimulated with 100 ng/ml of LPS. Samples of the culture media were taken at 0, 4 and 12 h of stimulation, and concentrations of TNF, IL-6, IL-12p40 and IL-12p70 were measured by a Luminex-based assay. Error bars represent the s.e.m of stimulations on independent cultures from 3 animals.

B) BMDMs from wild-type (WT) or MSK1,2 double knockout (KO) mice were stimulated with 100 ng/ml of LPS for the indicated times, and cells were lysed in SDS sample buffer. Cellular pre-TNF was measured by immunoblotting; total ERK1/2 is shown as a loading control. Plasma membrane-bound (extracellular) and intracellular TNF were measured by flow cytometry. WT BMDM, grey shaded histogram; MSK1,2 double knockout, black lines. Results are representative of at least three independent experiments.

C) BMDMs from either wild-type or MSK1,2 double knockout mice were stimulated with 100 ng/ml of LPS for the indicated times. Total RNA was then isolated and indicated transcripts were analyzed by qPCR. Samples were corrected for expression of 18s RNA and fold induction calculated relative to the wild-type 0 h time point. Error bars represent the s.e.m of stimulations on independent cultures from 3 animals.

Figure 3 MSKs regulate *Dusp1* transcription in macrophages.

A) BMDMs were isolated from wild-type (WT) and MSK1,2 double knockout (KO) mice. Cells were stimulated for the indicated times with 100 ng/ml of LPS. Total RNA was then isolated and DUSP1 mRNA expression analysed by qPCR. Results are corrected for 18s RNA expression and fold stimulation calculated relative to the wild-type 0 h time point. Error bars represent the s.e.m of stimulations on independent cultures from 3 animals.

B) Wild-type BMDMs were pre-incubated for 1 h with either PD184352 (2 μM), SB203580 (5 μM) or a combination of both inhibitors as indicated. Cells were then stimulated for 60 min with 100 ng/ml of LPS. Total RNA was isolated and DUSP1 mRNA expression was analysed by qPCR. Results are corrected for 18s RNA expression, and error bars represent the s.e.m of stimulations on independent cultures from 3 animals.

C) BMDMs from either wild-type or MSK1,2 double knockout mice were stimulated with LPS for the indicated times. Cells were lysed and immunoblotted for DUSP1, p-p38, total p38, p-ERK1/2 and total ERK1/2. Results are representative of 6 independent stimulations.

D) p-p38 and p-ERK1/2 immunoblots in (**c**) were quantified and corrected for total p38 and total ERK1/2, respectively, using the LI-CORR Odyssey detection system. Fold induction was calculated relative to the wild-type 0 h time point and error bars represent the s.e.m of six independent stimulations. $*P < 0.05$, $**P < 0.01$, wild-type versus MSK1,2 double knockout.

Figure 4 MSK regulates LPS-induced IL-10 production

A) BMDMs from wild-type (WT) and MSK1,2 double knockout (KO) mice were stimulated with 100 ng/ml of LPS for the indicated times. Total mRNA was isolated and IL-10 mRNA measured by qPCR. Samples were corrected for expression of 18s RNA and fold induction calculated relative to the wild-type 0 h time point. Error bars represent the s.e.m of stimulations on independent cultures from 3 animals.

B) As in (**a**), but concentrations of secreted IL-10 were measured by a Luminex-based assay. Error bars represent the s.e.m of stimulations on independent cultures from 3 animals.

C) BMDMs from wild-type (WT) or MSK1,2 double knockout (KO) mice were stimulated with 100 ng/ml of LPS for the indicated times and lysed in SDS sample buffer. p-STAT3(Tyr705), total STAT3, GAPDH and actin were measured using the LI-CORR Odyssey detection system. Bottom, representative immunoblots; top, quantification relative to an average of the GAPDH and actin loading controls. Error bars represent the s.e.m of stimulations on independent cultures from 3 animals.

D) BMDMs from wild-type or MSK1,2 double knockout mice were cultured and where indicated pre-treated for 15 min with either IL-10 or IL-6 neutralizing antibodies (2.5 μg/ml). Cells were then stimulated with either LPS (100 ng/ml, 8h), rmIL-10 (10 ng/ml, 30min) or rmIL-6 (10 ng/ml, 30min). Cells were then lysed and immunoblotted for p-STAT3(Tyr705) and total STAT3.

Figure 4 MSK induced IL-10 production inhibits IL-6 and IL-12 production.

A) BMDMs were pre-treated for 15 min with anti–IL-10 (2.5 μg/ml) or rat IgG (2.5 μg/ml) where indicated. Cells were stimulated with 100 ng/ml of LPS for 8 h. Cytokine concentrations in the media were measured by a Luminex-based assay. Error bars represent the s.e.m of stimulations on independent cultures from 3 animals.

B) As in (**e**) except total mRNA was isolated and indicated transcripts measured by qPCR. Samples were corrected for expression of 18s RNA and fold induction calculated relative to the wild-type 0 h time point. Error bars represent the s.e.m of stimulations on independent cultures from 3 animals.

C) BMDMs from wild-type, IL-10-deficient and MSK1,2,IL-10 triple knockout mice. Cells were stimulated with 100 ng/ml LPS and secreted cytokines were measured by a Luminex-based assay.

Figure 6 *Il10* and *Dusp1* promoters associate with p-CREB and/or p-ATF1.

A) Wild-type or MSK1,2 double knockout BMDMs were stimulated with 100 ng/ml LPS where indicated. Cells were fixed in formaldehyde and the chromatin fraction isolated. An antibody which recognizes p-CREB and p-ATF1 was used to immunoprecipitate chromatin. Input and immunoprecipitated chromatin was analysed by PCR using primers specific for the indicated promoters.

B) BMDMs isolated from control and CREB S133A mice were treated with 0.1 μM Tamoxifen from day 5 to 7 of differentiation. Macrophages were then replated in Tamoxifen-free media and used 24 h later. Cells were stimulated for the indicated times with 100 ng/ml LPS, lysed and analyzed by immunoblotting.

C) As in (**b**) except total RNA was isolated and indicated transcripts were measured by qPCR. 18s RNA was used as a loading control and fold stimulation calculated relative to wild-type control values. Error bars represent the s.e.m of 4 stimulations.

Figure 7 MSK1/2 in sensitivity to inflammation *in vivo*

A) Mice were implanted with a remote temperature sensor to allow continuous monitoring of body temperature. Two weeks later mice were injected i.p. with LPS (2.5 mg/kg) and their temperature recorded over time. Mice that showed a drop of approximately 2°C

below average diurnal temperature were sacrificed. Wild-type mice (*n*=6), MSK1,2 double knockout (*n*=5).

B) Wild-type (WT) and MSK1,2 double knockout (KO) mice were given an i.p. injection of either saline (control) or 1.8 mg/kg of LPS. Mice were sacrificed 1 or 4 h after injection and blood taken by cardiac puncture. Plasma cytokines were measured by a Luminex-based assay. Error bars represent the s.e.m of 6 mice.

C) Mice were subjected to cecal ligation and puncture or sham treated as described in the methods. Survival of mice was measured at the indicated times. Wild-type (*n*=10), MSK1,2 double knockout (*n*=10), sham (*n*=5). Animals were terminated if they were either moribound with a body temperature of 30^{o}C or if their temperature remained below 30^{o}C for 2 h.

D) Wild-type or MSK1,2 double knockout animals were subject to cecal ligation and puncture or shame treatment. Blood samples were taken at 1 and 4 hours, and plasma cytokine concentrations determined as described in the methods. MSK1,2 double knockouts (*n*=7), wild-type (*n*=7), sham (*n*=4). Error bars represent s.e.m.

Figure 8 MSK1,2 in sensitivity to PMA-induced eczema

A) Wild-type (WT) and MSK1,2 double knockout (KO) mice were treated with PMA (2.5 μg/ear) or vehicle (acetone) on the ears. Ear thickness was recorded over time. PMA-treated wild-type mice (*n*=12), PMA-treated MSK1,2 double knockout (*n*=12), vehicle-treated wild-type mice (*n*=8), and vehicle-treated MSK1,2 double knockout (*n*=8). Results are presented as mean ± s.e.m.

B) PMA (2.5 μg/ear) was applied to the ears of wild-type and MSK1,2 double knockout mice for the indicated time periods. 4 mm punch biopsies were taken from the ears and analysed for MPO activity (neutrophils ($\times 10^3$)/4 mm punch biopsy). PMA-treated wild-type mice (*n*=12), PMA-treated MSK1,2 double knockout mice (*n*=12), vehicle-treated

wild-type mice (*n*=8), and vehicle-treated MSK1,2 double knockout mice (*n*=8). Results are shown as mean ± s.e.m.

C) Haematoxylin and eosin-stained histological sections of wild-type and MSK1,2 double knockout mice treated with PMA (2.5 μg/ear) or vehicle for 72 h and 96 h. Scale bar = 100 μm. Representative transversal sections of vehicle-treated (*n*= 4) and PMA-treated (*n*=8) ears.

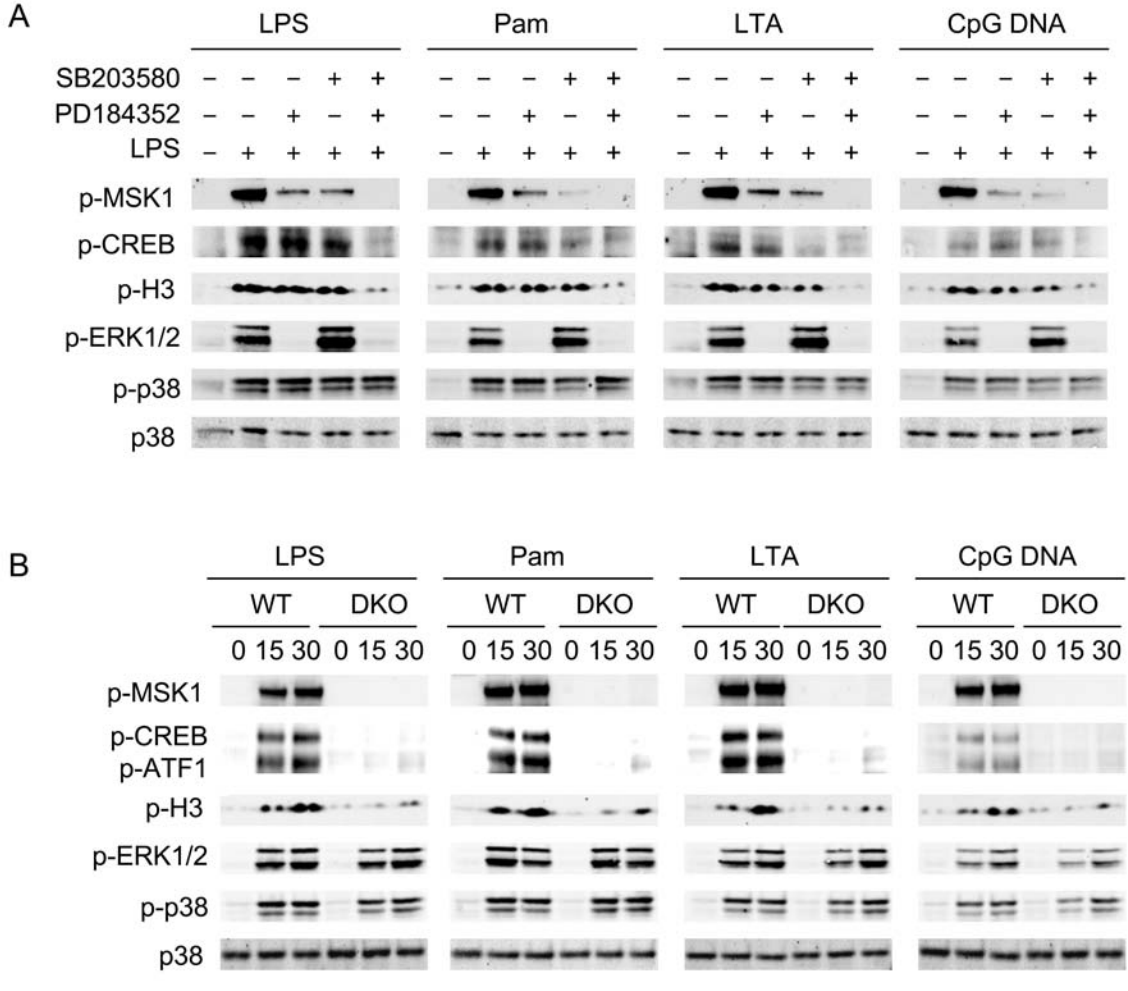
A
LPS
Pam
LTA
CpG DNA
SB203580
PD184352
LPS
p-MSK1
p-CREB
p-H3
p-ERK1/2
p-p38
p38
B
LPS
Pam
LTA
CpG DNA
WT
DKO
0 15 30
p-MSK1
p-CREB
p-ATF1
p-H3
p-ERK1/2
p-p38
p38

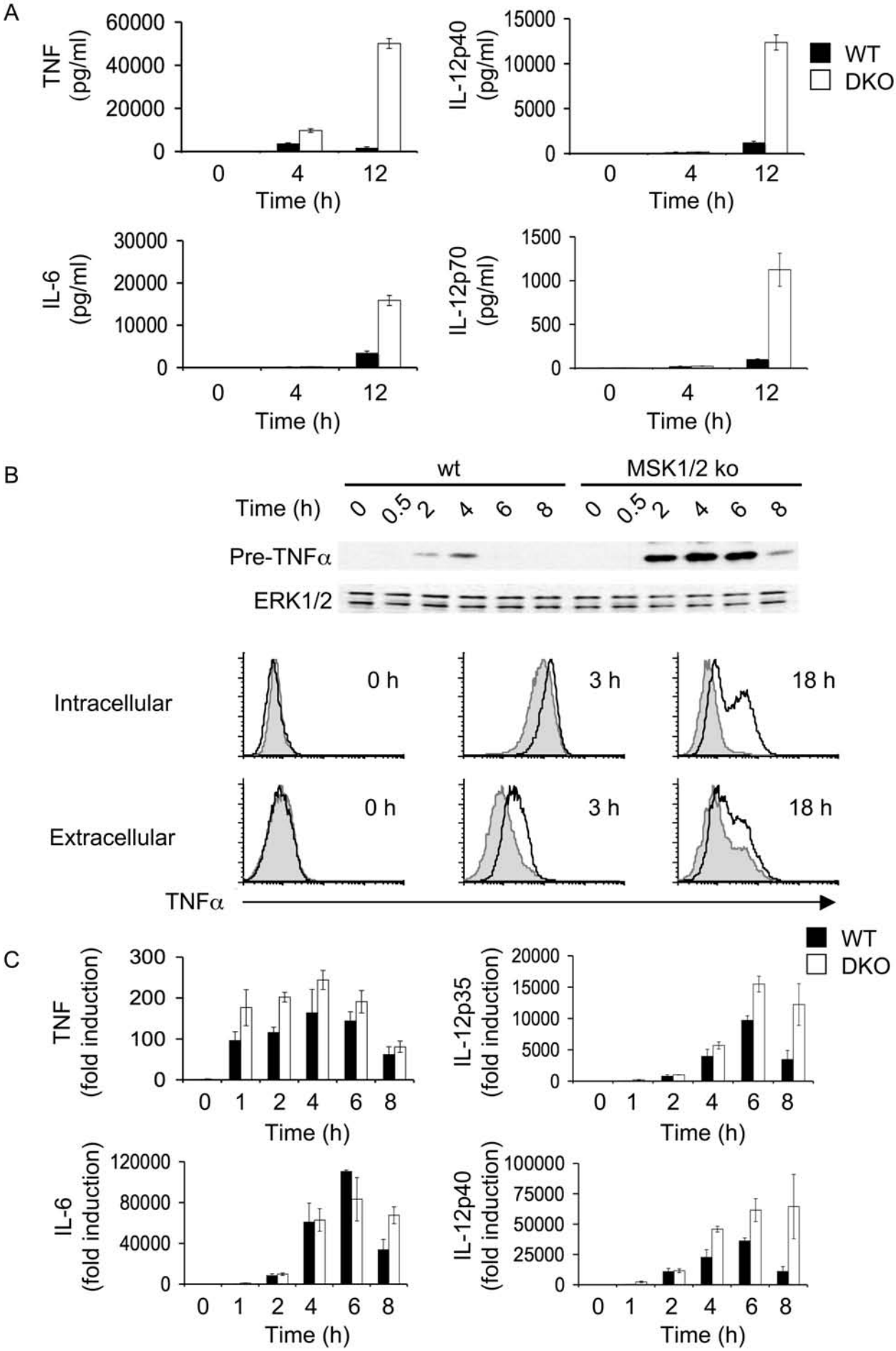
A
TNF (pg/ml)
60000
40000
20000
0
0
4
12
Time (h)
IL-12p40 (pg/ml)
15000
10000
5000
0
0
4
12
Time (h)
WT
DKO
IL-6 (pg/ml)
30000
20000
10000
0
0
4
12
Time (h)
IL-12p70 (pg/ml)
1500
1000
500
0
0
4
12
Time (h)
B
wt
MSK1/2 ko
Time (h)
0
0.5
2
4
6
8
0
0.5
2
4
6
8
Pre-TNFα
ERK1/2
Intracellular
Extracellular
0 h
3 h
18 h
0 h
3 h
18 h
TNFα
C
WT
DKO
TNF (fold induction)
300
200
100
0
0
1
2
4
6
8
Time (h)
IL-12p35 (fold induction)
20000
15000
10000
5000
0
0
1
2
4
6
8
Time (h)
IL-6 (fold induction)
120000
80000
40000
0
0
1
2
4
6
8
Time (h)
IL-12p40 (fold induction)
100000
75000
50000
25000
0
0
1
2
4
6
8
Time (h)

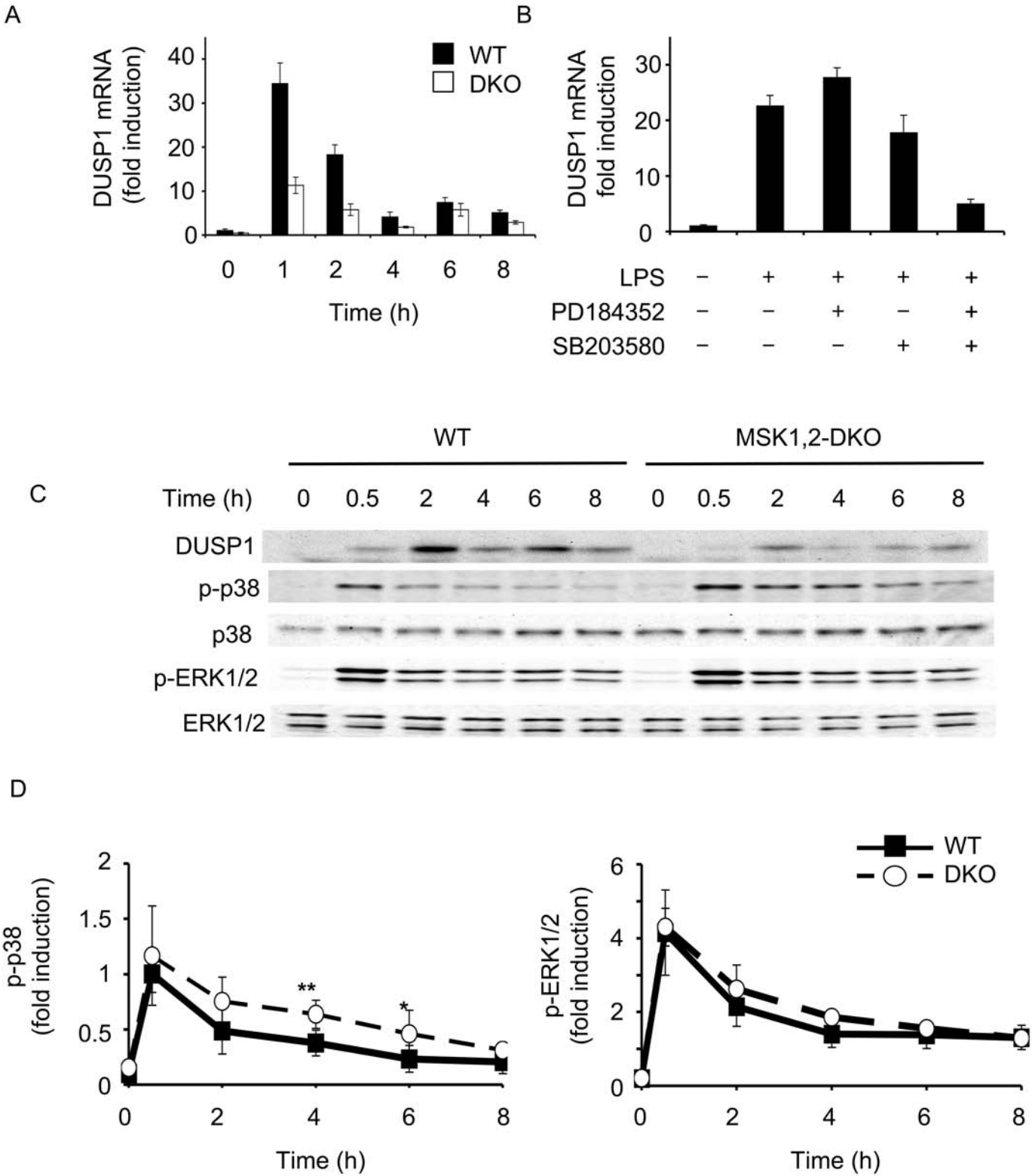
A
DUSP1 mRNA (fold induction)
40
30
20
10
0
WT
DKO
0 1 2 4 6 8
Time (h)
B
DUSP1 mRNA fold induction
30
20
10
0
LPS – + + + +
PD184352 – – + – +
SB203580 – – – + +
C
WT
MSK1,2-DKO
Time (h) 0 0.5 2 4 6 8 0 0.5 2 4 6 8
DUSP1
p-p38
p38
p-ERK1/2
ERK1/2
D
p-p38 (fold induction)
2
1.5
1
0.5
0
**
*
0 2 4 6 8
Time (h)
p-ERK1/2 (fold induction)
6
4
2
0
WT
DKO
0 2 4 6 8
Time (h)

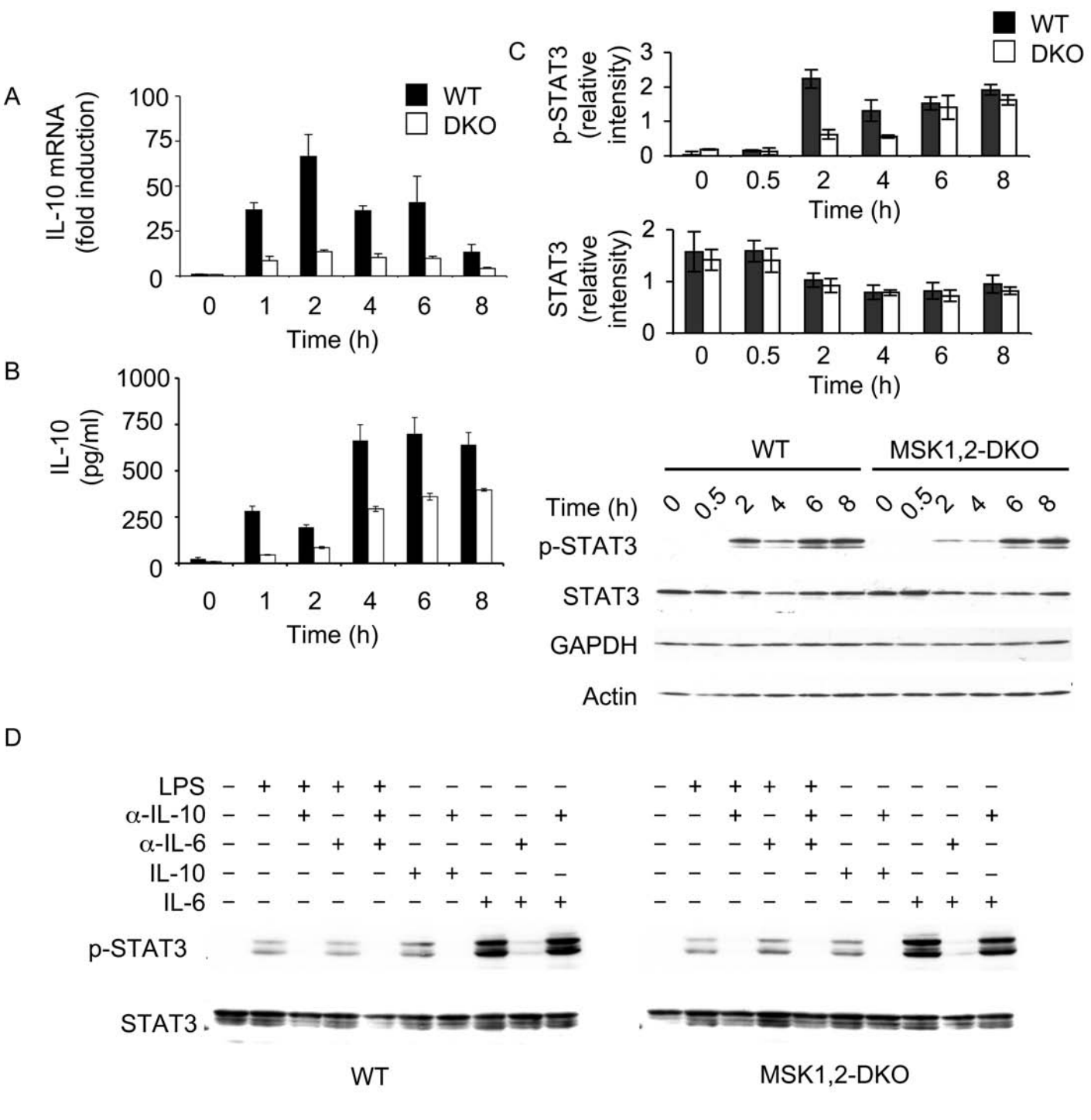
A
IL-10 mRNA (fold induction)
100
75
50
25
0
WT
DKO
0 1 2 4 6 8
Time (h)
B
IL-10 (pg/ml)
1000
750
500
250
0
0 1 2 4 6 8
Time (h)
C
WT
DKO
p-STAT3 (relative intensity)
3
2
1
0
0 0.5 2 4 6 8
Time (h)
STAT3 (relative intensity)
2
1
0
0 0.5 2 4 6 8
Time (h)
WT
MSK1,2-DKO
Time (h)
0 0.5 2 4 6 8 0 0.5 2 4 6 8
p-STAT3
STAT3
GAPDH
Actin
D
LPS
α-IL-10
α-IL-6
IL-10
IL-6
p-STAT3
STAT3
WT
MSK1,2-DKO

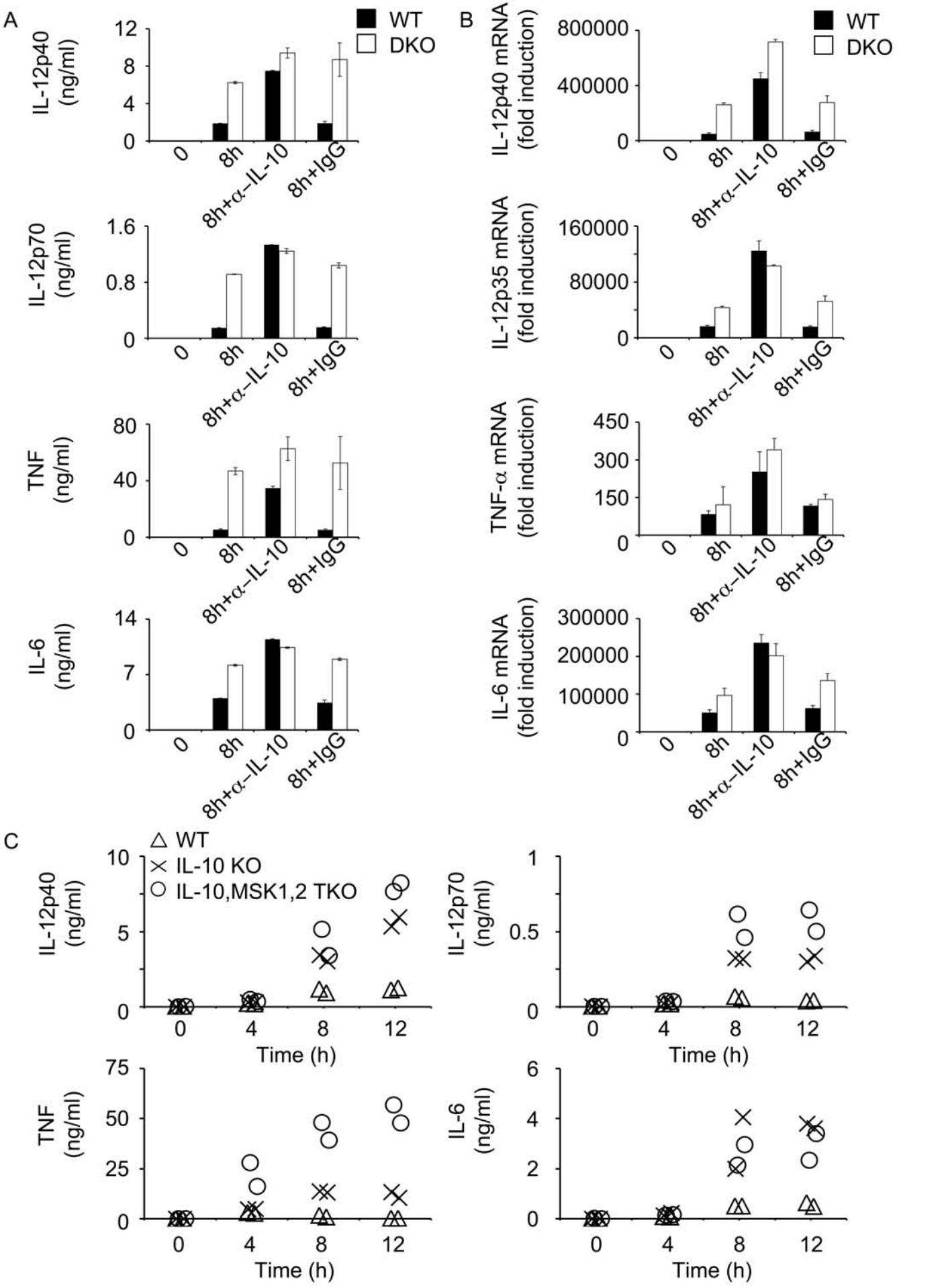
A
WT
DKO
IL-12p40 (ng/ml)
IL-12p70 (ng/ml)
TNF (ng/ml)
IL-6 (ng/ml)
0
8h
8h+α–IL-10
8h+IgG
B
IL-12p40 mRNA (fold induction)
IL-12p35 mRNA (fold induction)
TNF-α mRNA (fold induction)
IL-6 mRNA (fold induction)
C
WT
IL-10 KO
IL-10,MSK1,2 TKO
Time (h)

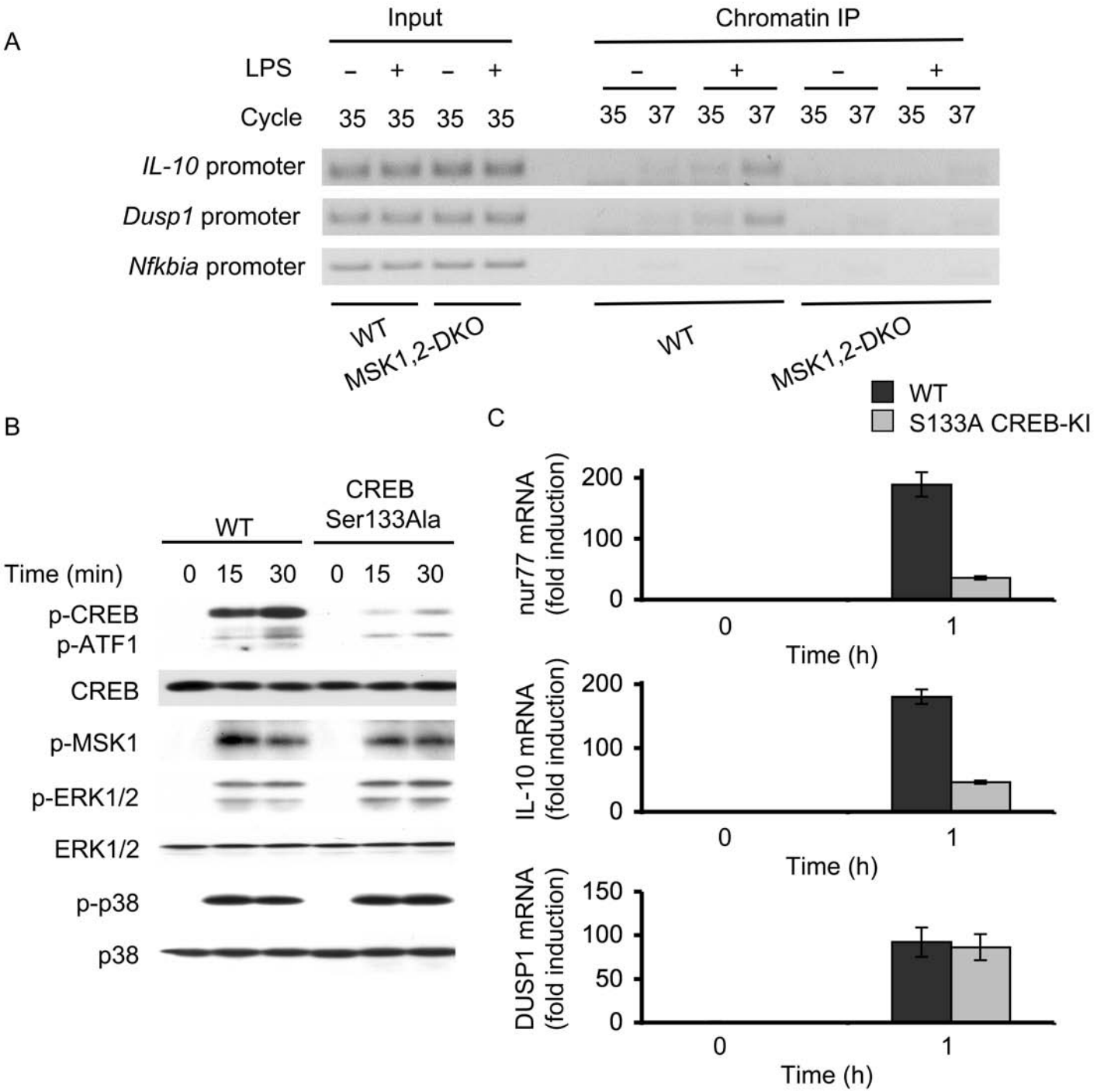
A
Input
Chromatin IP
LPS
– + – +
– + – +
Cycle
35 35 35 35
35 37 35 37 35 37 35 37
IL-10 promoter
Dusp1 promoter
Nfkbia promoter
WT
MSK1,2-DKO
WT
MSK1,2-DKO
B
WT
CREB Ser133Ala
Time (min)
0 15 30 0 15 30
p-CREB
p-ATF1
CREB
p-MSK1
p-ERK1/2
ERK1/2
p-p38
p38
C
WT
S133A CREB-KI
nur77 mRNA (fold induction)
200
100
0
0
1
Time (h)
IL-10 mRNA (fold induction)
200
100
0
0
1
Time (h)
DUSP1 mRNA (fold induction)
150
100
50
0
0
1
Time (h)

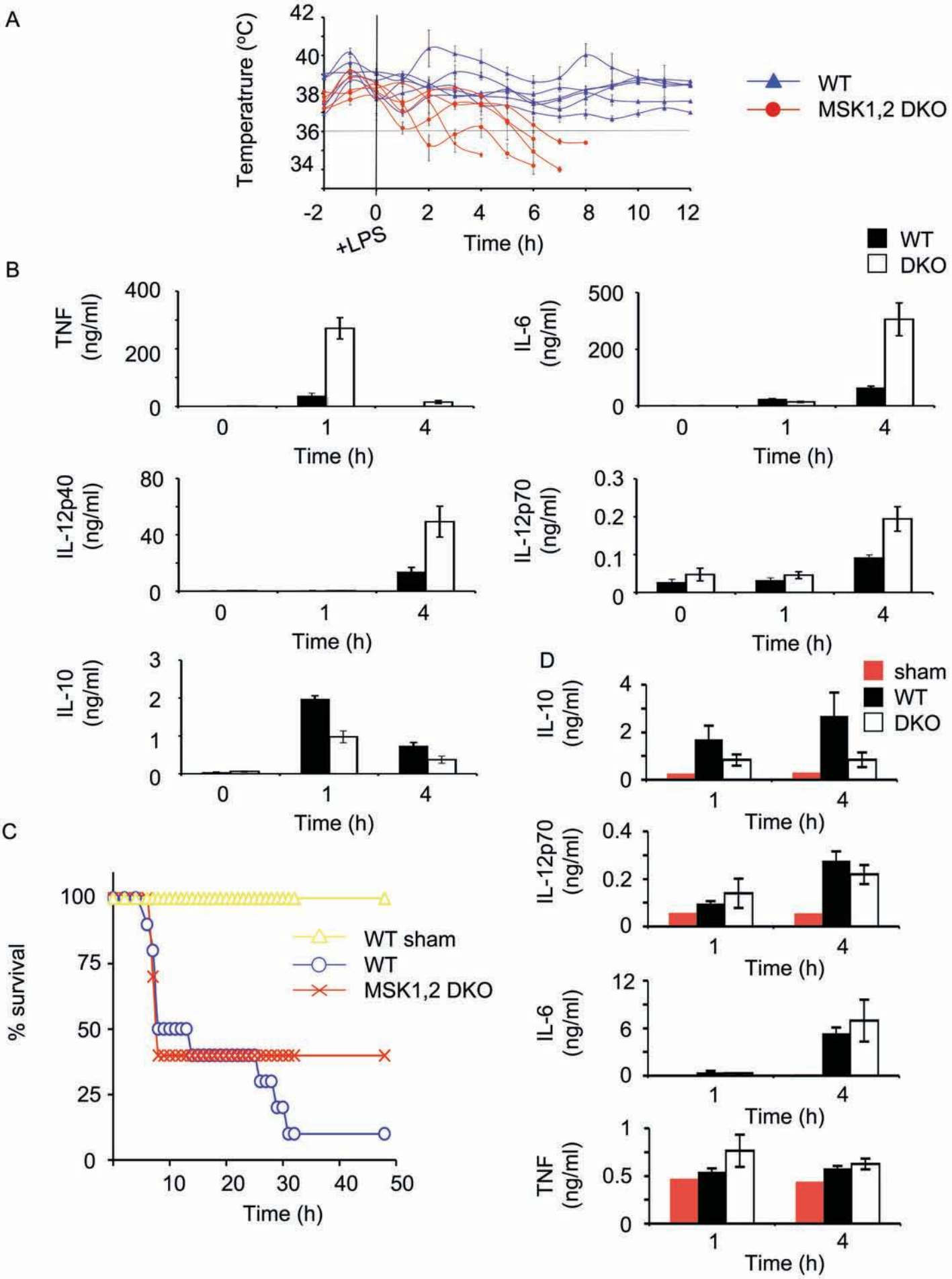
A
Temperature (°C)
42
40
38
36
34
-2
0
2
4
6
8
10
12
+LPS
Time (h)
WT
MSK1,2 DKO
B
WT
DKO
TNF (ng/ml)
400
200
0
IL-6 (ng/ml)
500
200
0
IL-12p40 (ng/ml)
80
40
0
IL-12p70 (ng/ml)
0.3
0.2
0.1
0
IL-10 (ng/ml)
3
2
1
0
0
1
4
Time (h)
C
% survival
100
75
50
25
0
10
20
30
40
50
Time (h)
WT sham
WT
MSK1,2 DKO
D
sham
WT
DKO
IL-10 (ng/ml)
4
2
0
IL-12p70 (ng/ml)
0.4
0.2
0
IL-6 (ng/ml)
12
6
0
TNF (ng/ml)
1
0.5
0
1
4
Time (h)

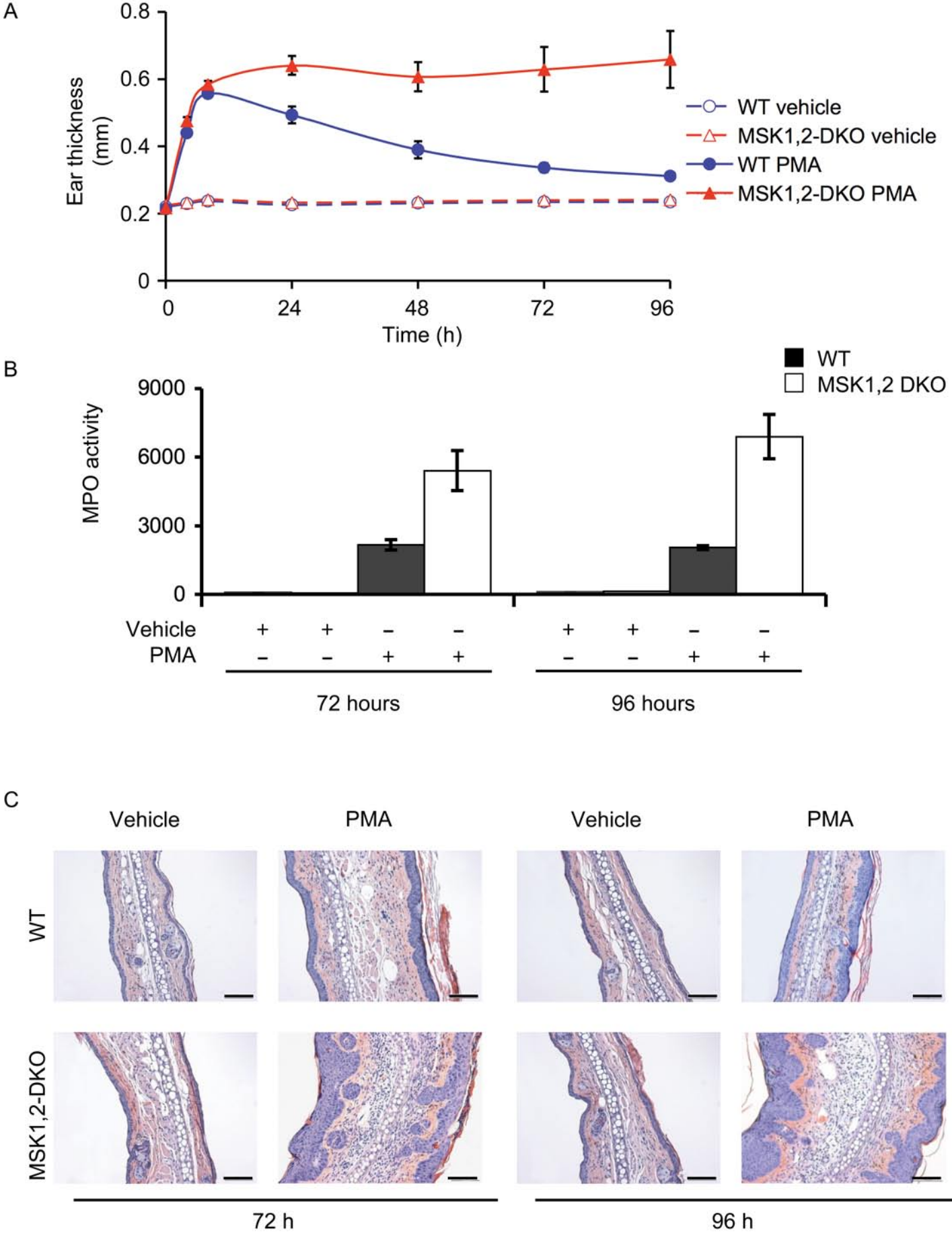
A
Ear thickness (mm)
0.8
0.6
0.4
0.2
0
0
24
48
72
96
Time (h)
WT vehicle
MSK1,2-DKO vehicle
WT PMA
MSK1,2-DKO PMA
B
WT
MSK1,2 DKO
MPO activity
9000
6000
3000
0
Vehicle
PMA
72 hours
96 hours
C
Vehicle
PMA
Vehicle
PMA
WT
MSK1,2-DKO
72 h
96 h

Supplementary methods

Antibodies

Anti-ERK1/2, anti-p-ERK1/2, anti-p38 anti-p-MSK1 (Thr581) and anti-p-MSK2 polyclonal were from Cell Signalling and the anti-p-Histone H3(Ser10) antibody was from Upstate. The monoclonal anti-p-CREB(Ser133) (clone 10E9) was from Upstate. Rat anti-mouse IL-10R was kindly provided by Ann O'Garra (National Institute of Medical Research, London). The polyclonal anti-PreTNF and anti–IL-6 antibodies were from R&D Systems (AF-410-NA; AF-406-NA). Antibodies for FACS analysis (anti-TNF-PE clone MP6-XT22, anti-F4/80-FITC clone BM8 and anti-CD83-PE clone Michel-19) were purchased from Serotec and BD Pharmingen, respectively.

Real-time PCR

Total RNA (0.5 μg) was reverse-transcribed using iSCRIPT cDNA synthesis kit (Bio-Rad). Real-time PCR was carried out using SYBRgreen detection kit (Bio-Rad) according to manufacturer's instructions. Fold changes in mRNA expression were quantified relative to unstimulated wild-type cells, and 18S RNA was used as a loading control as described[1]. Sequences for the primers are listed in **Supplementary Table 1**.

Multiplex cytokine assay

Cytokine concentrations in cell supernatants and mouse plasma samples were detected using either Luminex-based Bio-Plex ™ Mouse Grp I Cytokine 23-Plex Panel (Bio-Rad) or individual Bioplex cytokine kits.

FACS

BMDMs were stimulated with 100 ng/ml LPS for the indicated times and stained with anti-F4/80-FITC and anti-TNF-PE antibodies. For detection of intracellular TNF cells were stained using BD Cytofix/Cytoperm^{TM} Plus Fixation/Permeabilization Kit with BD GolgiPlug ^{TM}. Prior to detection of extracellular TNF cells were pre-treated for 6 h with 1 μg/ml TACE inhibitor (Calbiochem).

Histology

Skin samples were fixed in 4% formaldehyde, embedded in paraffin, and processed for histological analysis. Sections were cut at 4 μm, mounted onto slides, and stained with haematoxylin and eosin according to standard procedures.

Chromatin immunoprecipitation (ChIP)

Cells were fixed with formaldehyde, and chromatin was isolated and subjected to mechanical sheering and immunoprecipitation as described[2]. Anti-p-CREB (R&D Systems) was used to immunoprecipitate specific chromatin DNA fragments. The sequences of the promoter specific primers are shown in **supplementary table 1.**

Ser133Ala CREB conditional knockin mutation

A conditional knockin mutation of Ser133 to alanine was generated using a minigene method similar to that described in[3] and illustrated in **supplementary Fig. 7A**. In this method a minigene (driven of the endogenous promoter) is inserted upstream of the mutated exon, and results in transcription of a wild type protein. Expression of Cre recombinase excises the minigene due to the presence of flanking LoxP sites, and allows transcription of the mutated exon. In this study, mice homozygous for the

targeted CREB locus a Tamoxifen inducible Cre transgenic. These mice express a mutated ER-Cre fusion protein that is inactive in the absence of Tamoxifen[4]. Addition of Tamoxifen to BMDMs from these mice activates the Cre resulting in excision of the minigene. To determine the efficiency of excision in BMDMs, the CREB mRNA was subclonned and sequenced. This showed an efficiency of approximately 60% (25 mutated sequences out of 41, cloned from 4 independent reverse transcriptions). Primers used for PCR of CREB are given in supplementary table 1. Quantitative PCR analysis using the same primers showed that the relative expression level of the CREB mRNA between Ser133Ala knockin and wild-type cells was similar indicating that the mutation did not affect CREB mRNA levels in the cell (JSCA, data not shown).

Supplementary references

1. Darragh, J. et al. MSKs are required for the transcription of the nuclear orphan receptors Nur77, Nurr1 and Nor1 downstream of MAPK signalling. *Biochem J* **390**, 749-59 (2005).
2. Saccani, S. & Natoli, G. Dynamic changes in histone H3 Lys 9 methylation occurring at tightly regulated inducible inflammatory genes. *Genes Dev* **16**, 2219-24 (2002).
3. Bayascas, J.R., Sakamoto, K., Armit, L., Arthur, J.S. & Alessi, D.R. Evaluation of approaches to generation of tissue-specific knock-in mice. *J Biol Chem* **281**, 28772-81 (2006).
4. Seibler, J. et al. Rapid generation of inducible mouse mutants. *Nucleic Acids Res* **31**, e12 (2003).

Supplementary table 1. Primer sequences used for PCR.

symbol	protein	use	Sense primer	Antisense primer
Il12a	IL-12p35	q-PCR	TATCTCTATGGTCAGCGTTCC	TGGTCTTCAGCAGGTTTCG
Il12b	IL-12p40	q-PCR	TCATCAGGGACATCATCAAACC	TGAGGGAGAAGTAGGAATGGG
Tnf	TNFα	q-PCR	CAGACCCTCACACTCAGATCATC	GGCTACAGGCTTGTCACTCG
Il6	IL-6	q-PCR	TTCCATCCAGTTGCCTTCTTG	AGGTCTGTTGGGAGTGGTATC
Il10	IL-10	q-PCR	CCCTTTGCTATGGTGTCCTTTC	GATCTCCCTGGTTTCTCTTCCC
Dusp1	DUSP1	q-PCR	TGGGAGCTGGTCCTTATTTATT	GACTGCTTAGGAACTCAGTGGAA
18s	18s RNA	q-PCR	GTAACCCGTTGAACCCCATT	CCATCCAATCGGTAGTAGCG
Egr1	Egr1	q-PCR	ACAGAAGGACAAGAAAGCAGAC	CCAGGAGAGGAGTAGGAAGTG
Nr4a1	Nur77	q-PCR	CCTGTTGCTAGAGTCTGCCTTC	CAATCCAATCACCAAAGCCACG
Creb1	CREB	q-PCR	CCGGAACTCAGATTTCAACTATTGC	CCTCTTCTGACTTTTCTTCTTCAATCC
Dusp1	DUSP1	ChIP	GTCTTTGCTTTTGGCTTTGG	CGCGGTTTTATGTAGCCTCT
Il10	IL-10	ChIP	CAGAAGTTCATTCCGACCAGT	CCTTCCTGGCAAAGGTTTTT
Nfkbia	IκBα	ChIP	AAAGTTCCCTGTGCATGACC	GGAATTTCCAAGCCAGTCAG

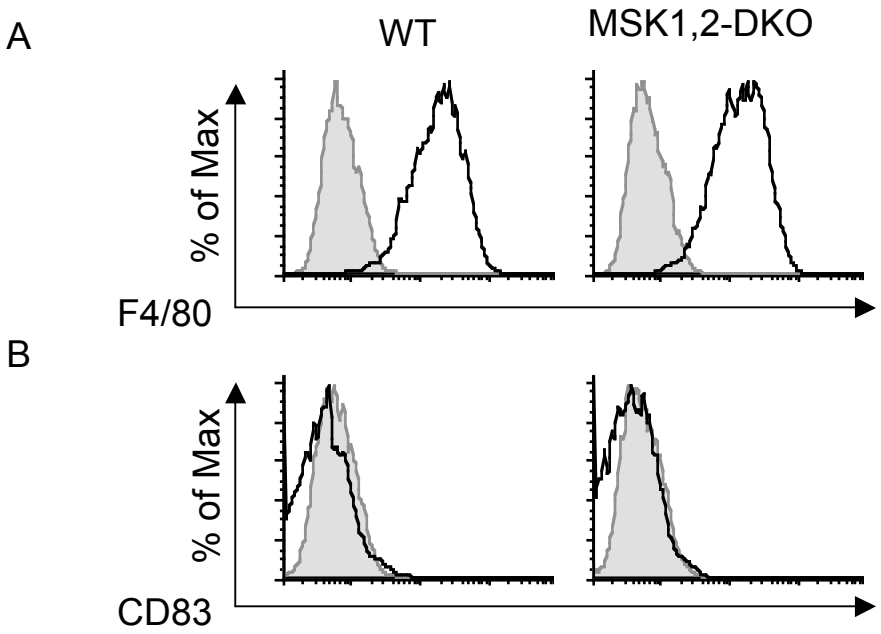

Supplementary Figure 1. Knockout of MSK1 and MSK2 does not affect macrophage differentiation.

A) Bone marrow cells were differentiated into BMDMs by culturing for seven days in media containing 5 ng/ml M-CSF. Cultured cells were stained with an antibody specific for the macrophage marker F4/80 (black lines). Isotype control staining is shown by the shaded grey area.

B) As in (A), but cells were stained with an antibody specific for the dendritic cell marker CD83 to control for dendritic cell contamination.

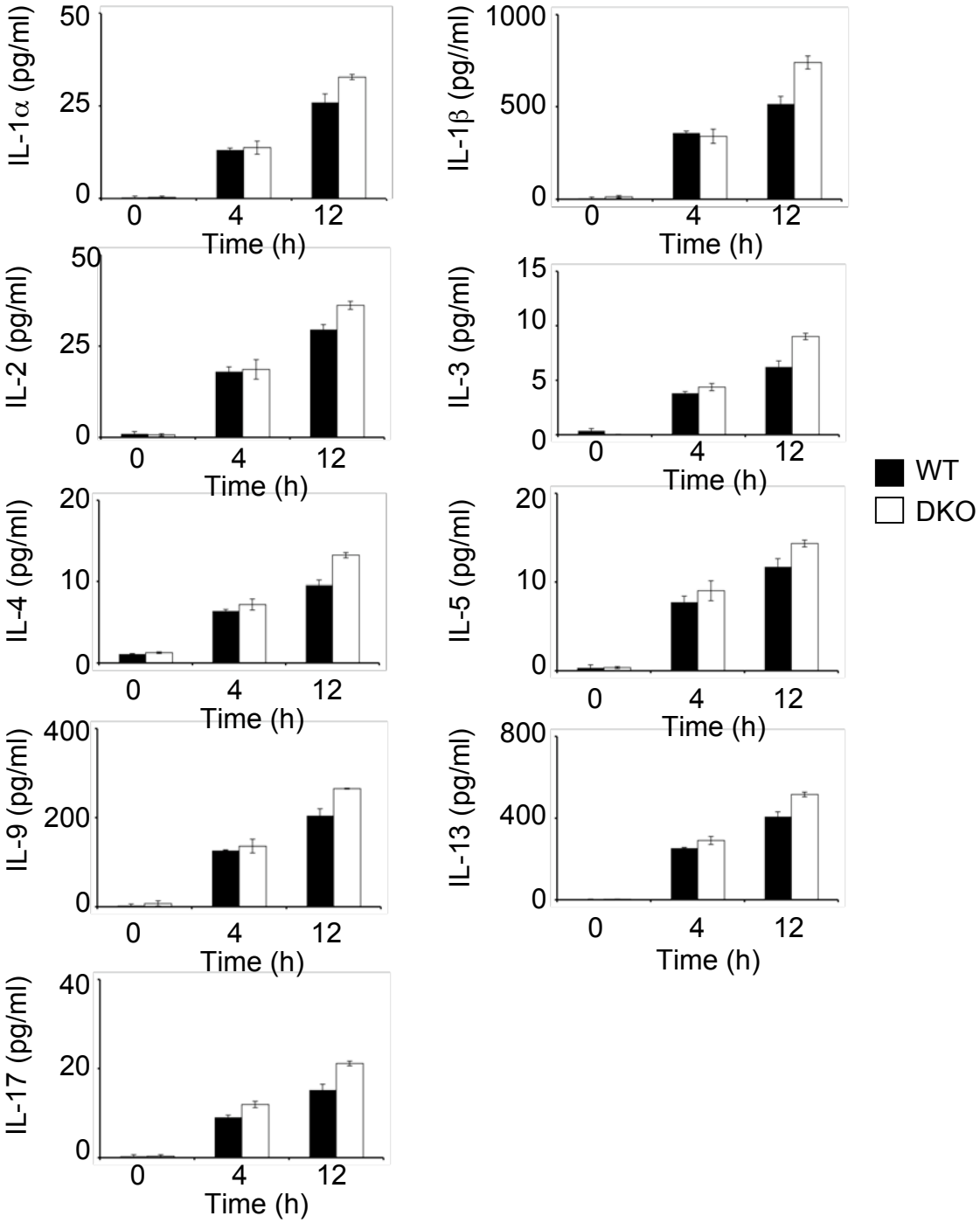

Supplementary Figure 2. No difference in the production of cytokines IL-1α, IL-1β, IL-2, IL-3, IL-4, IL-5, IL-9, IL-13 and IL-17 by wild-type and MSK1,2 knockout cells.
BMDMs from either wild-type or MSK1,2 knockout mice were stimulated with 100 ng/ml of LPS. Samples of the culture media were taken at 0, 4 and 12 hours after stimulation, and the concentrations were measured by a Luminex-based assay. Error bars represent the s.e.m of three independent stimulations.

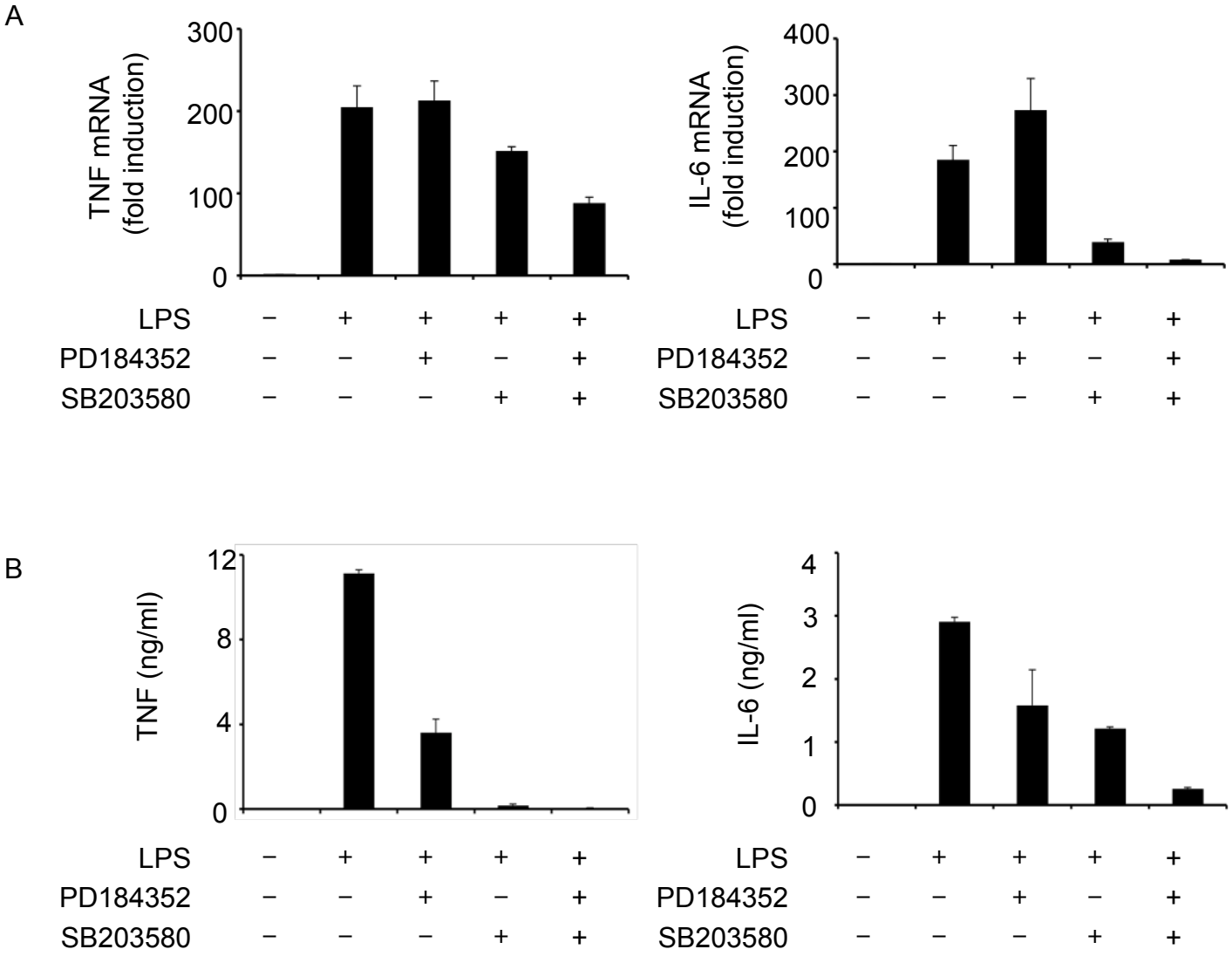

Supplementary Figure 3. ERK1/2 and p38 regulate TNF and IL-6 production.

A) Wild type BMDMs were pre-incubated for 1 h with either PD184352 (2 μM), SB203580 (5 μ M) or a combination of both inhibitors as indicated. Cells were then stimulated for 60 min with 100 ng/ml of LPS. Total RNA was isolated and TNF or IL-6 mRNA expression analyzed by PCR. Results are corrected for 18s RNA quantities, and error bars represent the s.e.m of three independent stimulations.

B) Wild type BMDMs were pre-incubated for 1 h with either PD184352 (2 μM), SB203580 (5 μ M) or a combination of both inhibitors as indicated. Cells were then stimulated for 6 h with 100 ng/ml of LPS. Concentrations of secreted TNF and IL-6 were measured by a Luminex-based assay. Error bars represent the s.e.m of three independent stimulations.

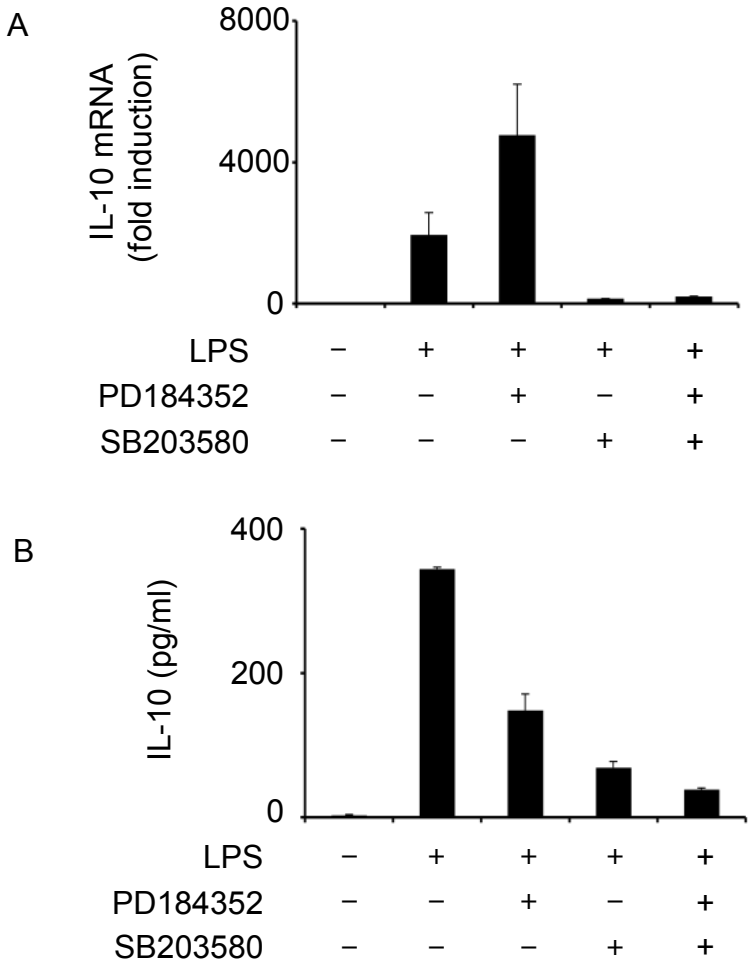

Supplementary Figure 4. Both ERK1/2 and p38 regulate production of IL-10.

A) Wild type BMDMs were pre-incubated for 1 h with either PD184352 (2 μM), SB203580 (5 μ M) or a combination of both inhibitors as indicated. Cells were then stimulated for 60 min with 100 ng/ml of LPS. Total RNA was isolated and IL-10 mRNA expression analyzed by PCR. Results are corrected for 18s RNA quantities, and error bars represent the s.e.m of three independent stimulations.

B) Wild type BMDMs were pre-incubated for 1 h with either PD184352 (2 μM), SB203580 (5 μ M) or a combination of both inhibitors as indicated. Cells were then stimulated for 6 h with 100 ng/ml of LPS. Concentrations of secreted IL-10 were measured by a Luminex-based assay. Error bars represent the s.e.m of three independent stimulations.

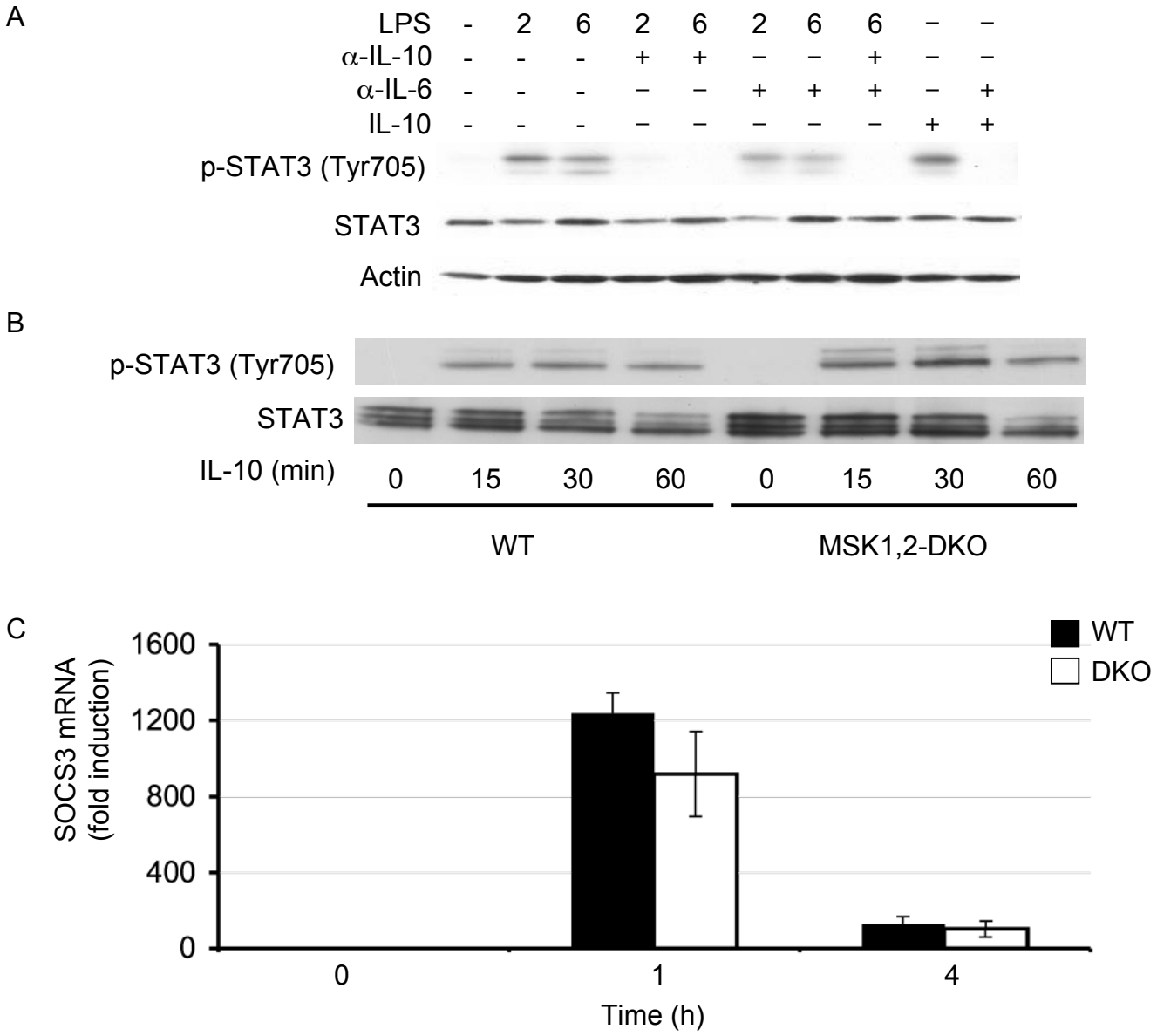

Supplementary Figure 5. IL-10-induced STAT3 phosphorylation is MSK-independent.

A) Wild-type BMDMs were pretreated for 15 min with either α-IL-10 or α-IL-6 neutralising antibodies (2.5 μg/ml) where indicated. Cells were then stimulated with either LPS (100 ng/ml, 2 or 6 h) or rmIL-10 (10 ng/ml, 30 min). Cells were lysed and immunoblotted for phosphorylated STAT3 (Tyr705) , total STAT3 and actin.

B) BMDMs were isolated from wild-type or MSK1,2 knockout mice and stimulated with IL-10 (10 ng/ml) for the indicated times. Cells were lysed and immunoblotted for phosphorylated STAT3 (Tyr705) and total STAT3.

C) Total RNA was isolated from wild-type (black bars) or MSK1,2 knockout (white bars) following LPS stimulation for the indicated times. SOCS3 mRNA quantities were determined using 18s RNA as a loading control by quantitative-PCR. Error bars represent the s.e.m. of 6 stimulations.

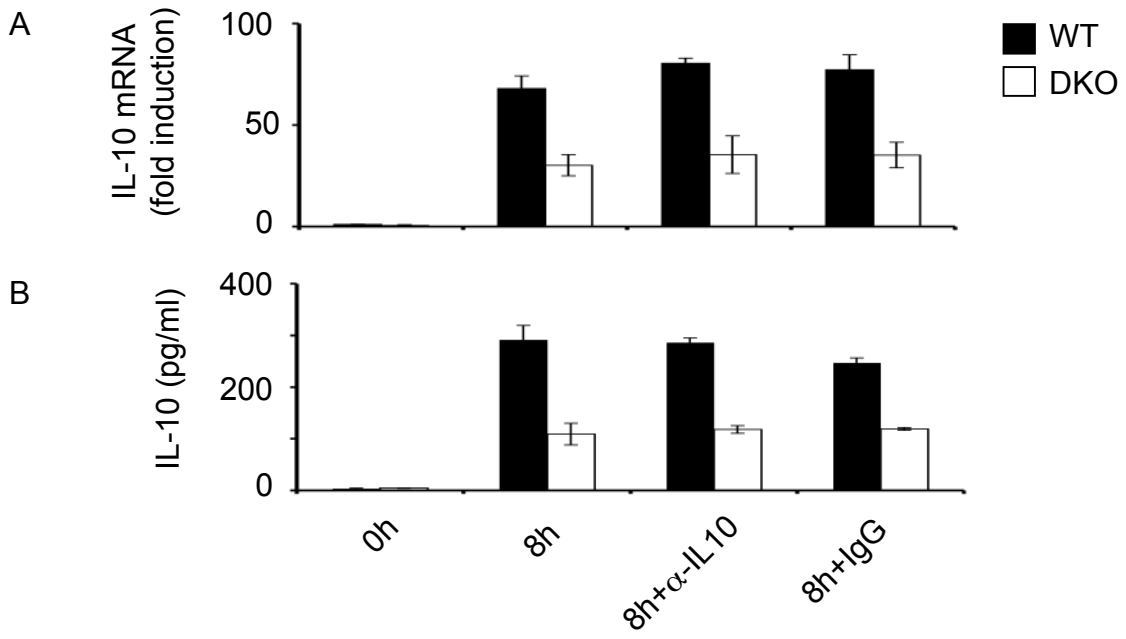

Supplementary Figure 6. IL-10 production is not affected by IL-10- neutralizing antibodies.

A) BMDMs were pre-treated for 15 min with anti-IL10 (2.5 μg/ml) or rat IgG (2.5 μg/ml) as indicated. Cells were stimulated with 100 ng/ml of LPS for 8 h. Cells were lysed and total mRNA was isolated. IL-10 mRNA quantities were determined by PCR. Samples were corrected for expression of 18s RNA and fold induction calculated relative to the wild type zero time point. Error bars represent the s.e.m of three independent stimulations.

B) As in (A) except concentrations of IL-10 secreted into the media were measured by a Luminex-based assay. Error bars represent the s.e.m of three independent stimulations.

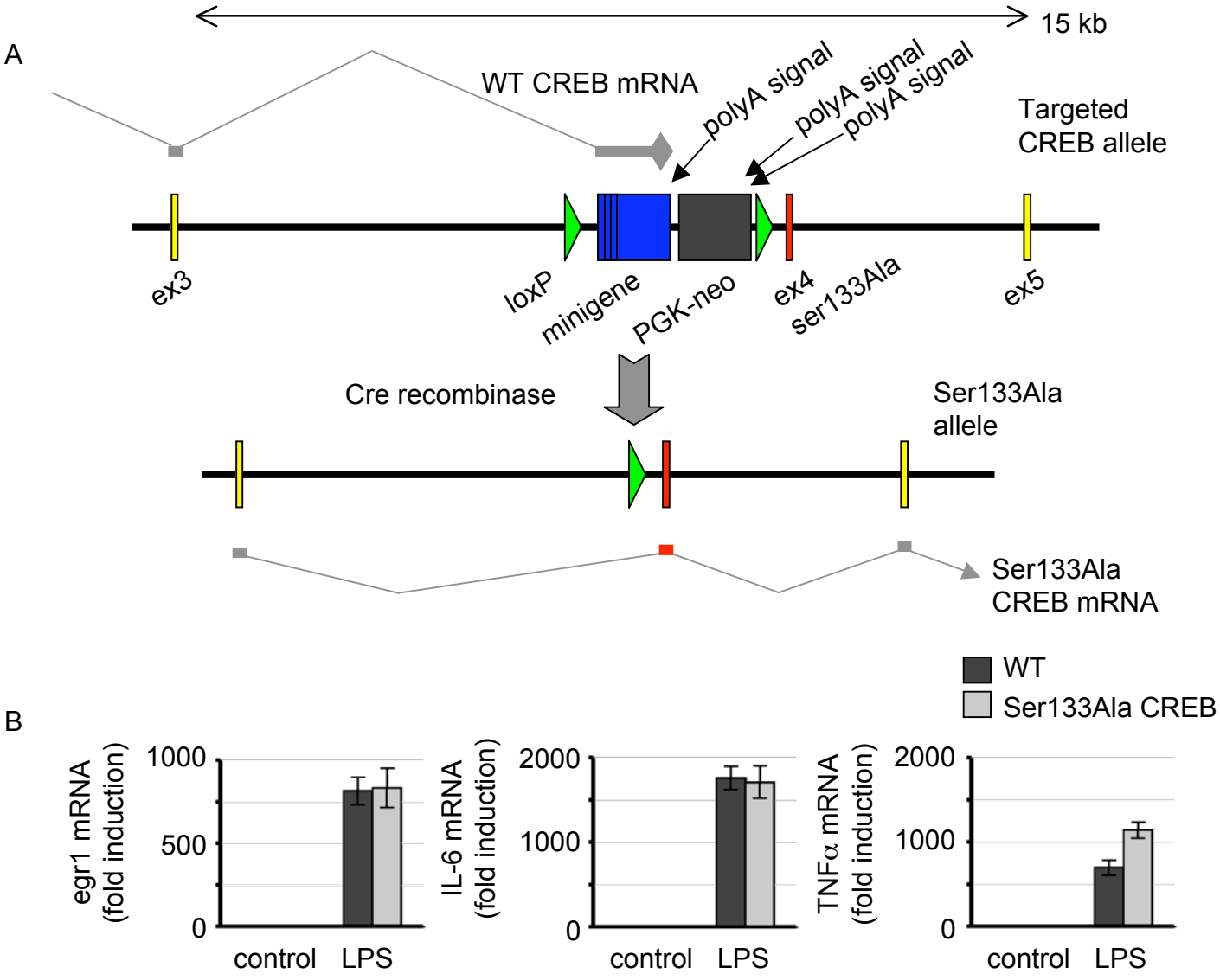

Supplementary Figure 7. Ser133Ala CREB knockin BMDMs

A) To create a conditional CREB Ser133Ala allele, a CREB minigene (blue) and a mutated version on exon 4 (containing the Ser133Ala mutation) were introduced in place of exon 4 of the endogenous CREB gene using conventional gene targeting techniques. The minigene contained a wild type exon 4 sequence fused to the 3' exons of the CREB gene. To allow selection in embryonic stem cells, it was followed by a PGK-neomycin cassette. Both the CREB minigene and neo were followed by polyadenylation sequences to terminate transcription. To allow excision, the mini gene was flanked by loxP sites (green triangles). Predicted splicing is shown by grey lines. In the targeted allele, splicing should occur onto the minigene, resulting in a wild type protein. Following expression of Cre, the minigene is removed allowing splicing onto the mutated exon 4 and transcription of the Ser133Ala mutant. To achieve deletion in macrophage culture, mice were crossed on to a tamoxifen inducible CRE transgenic background.

B) BMDMs were isolated from wild type (black bars) and CREB Ser133Ala knockin (grey bars) mice. Both cultures were treated with 0.1 μM Tamoxifen from day 5 to 7 of differentiation. Macrophages were then replated in Tamoxifen free media and used 24 h later. Cells were stimulated for 1 hour with 100 ng/ml LPS or left unstimulated. Total RNA was isolated and the quantities the CREB independent gene egr1, as well as TNFα and IL-6 were determined by quantitative-PCR. 18s RNA was used as a loading control and fold induction calculated relative to wild-type control values. Error bars represent the s.e.m of 4 stimulations.

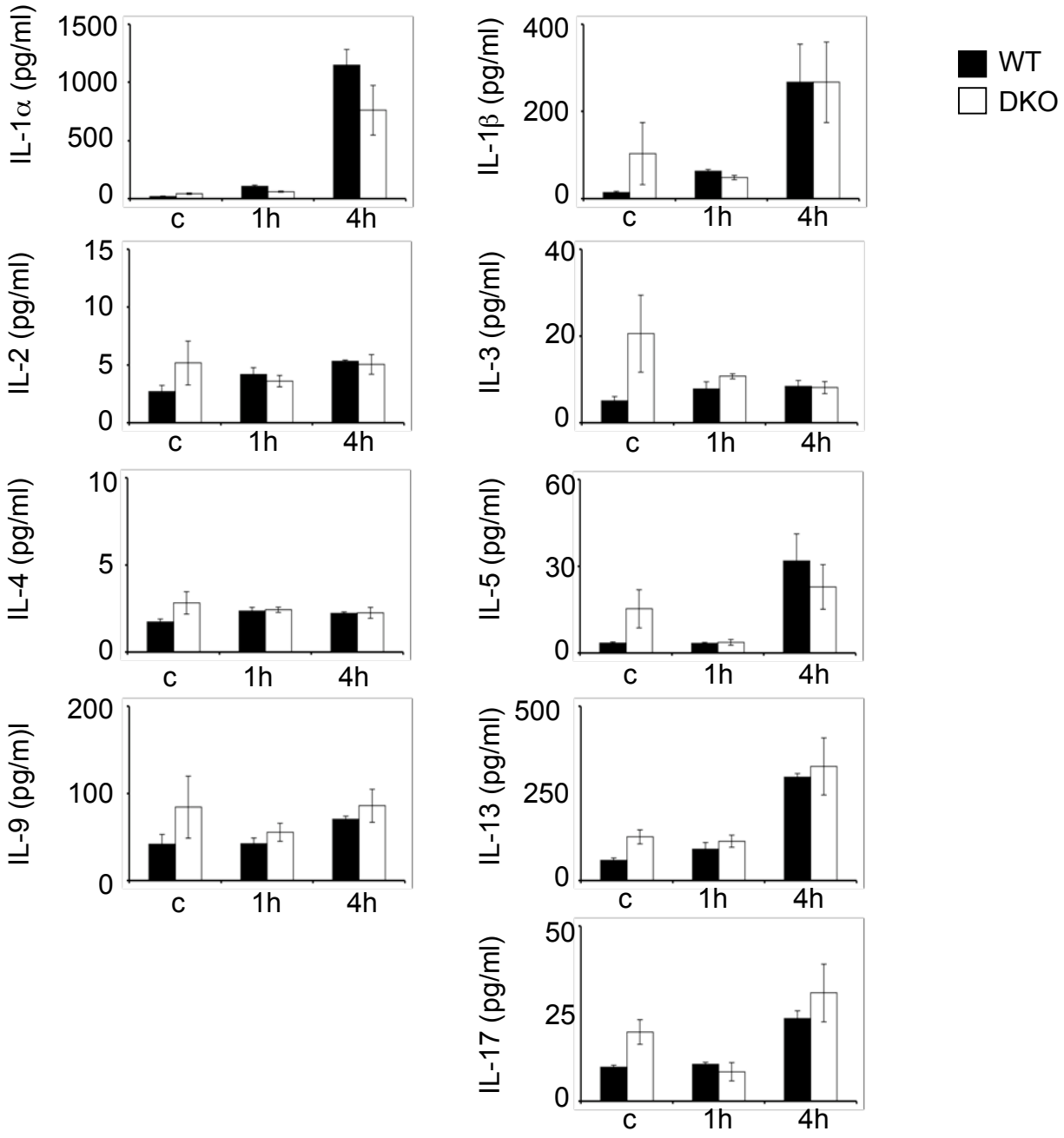

Supplementary Figure 8. Plasma cytokine concentrations following an i.p. injection of LPS.
Wild-type (black bars) and MSK1,2 knockout (white bars) mice were given an i.p. injection of either saline control (c) or 1.8 mg/kg of LPS for 1 h or 4 h. Mice were sacrificed and blood taken by cardiac puncture. Plasma cytokine concentrations were measured by a Luminex-based assay. Error bars represent the s.e.m of 6 mice.

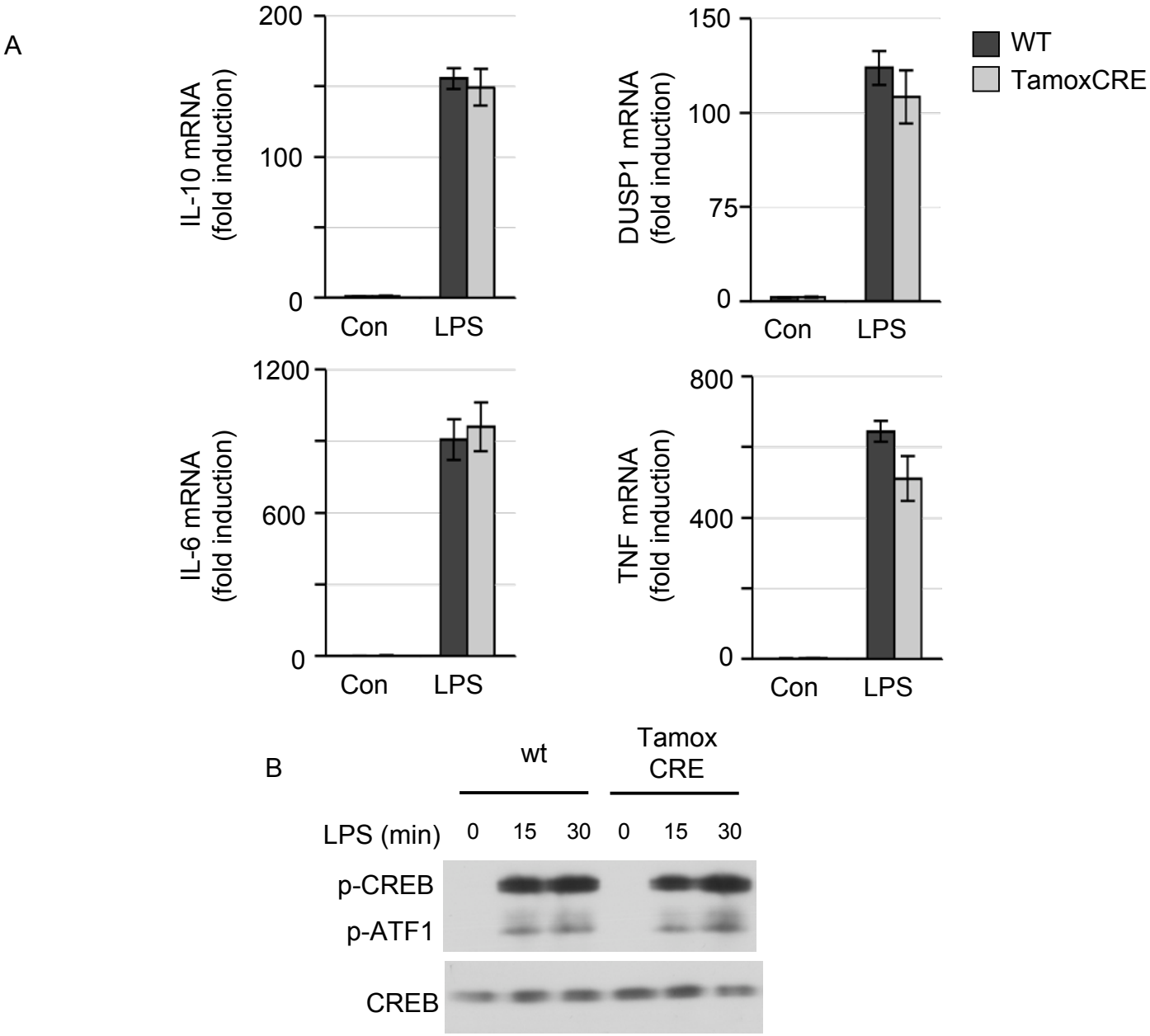

Supplementary Figure 9. Tamoxifen CRE does not affect LPS-induced CREB phosphorylation or cytokine transcription.

A) BMDMs were isolated from wild type (black bars) and Tamoxifen-CRE (grey bars) mice. Both cultures were treated with 0.1 μM Tamoxifen from day 5 to 7 of differentiation. Macrophages were then replated in Tamoxifen free media and used 24 h later. Cells were stimulated for 1 hour with 100 ng/ml LPS or left unstimulated. Total RNA was isolated and the quantities of IL-10, DUSP1, IL-6 and TNFα were determined by quantitative-PCR. 18s was used as a loading control and fold stimulation calculated relative to wild type control values. Error bars represent the s.e.m of 4 stimulations.

B) As (A) except that cells were stimulated for 15 or 30 min with LPS and then lysed into SDS sample buffer. Levels of phosphorylated CREB (Ser133) and total CREB were determined by immunoblotting